Development of the DRoplet Ice Nuclei Counter Zürich (DRINCZ): Validation and application to field collected snow samples

Robert O. David[1,*], Maria Cascajo-Castresana[1,2], Killian P. Brennan[1], Michael Rösch[1], Nora Els[4], Julia Werz[3], Vera Weichlinger[1], Lin S. Boynton[3], Sophie Bogler[3], Nadine Borduas-Dedekind[1,3], Claudia Marcolli[1], Zamin A. Kanji[1]

[1]Institute of Atmospheric and Climate Science, ETH Zürich, Zürich, 8092, Switzerland
[2]CIC nanoGUNE Consolider, Donostia-San Sebastian, E-20018, Spain
[3]Institute for Biogeochemistry and Pollutant Dynamics, ETH Zürich, Zürich, 8092, Switzerland
[4]Institute of Ecology, University of Innsbruck, Innsbruck, 6020, Austria
*Now at Department of Geosciences, University of Oslo, Oslo, 0315, Norway

Correspondence to: Robert O. David (r.o.david@geo.uio.no) and Zamin A. Kanji (zamin.kanji@env.ethz.ch)

Abstract. Ice formation in the atmosphere is important for regulating cloud lifetime, Earth's radiative balance and initiating precipitation. Due to the difference in the saturation vapor pressure over ice and water, in mixed-phase clouds (MPCs), ice will grow at the expense of supercooled cloud droplets. As such, MPCs, which contain both supercooled liquid and ice, are particularly susceptible to ice formation. However, measuring and quantifying the concentration of ice nucleating particles (INPs) responsible for ice formation at temperatures associated with MPCs is challenging due to their very low concentrations in the atmosphere (~ 1 in 10^5 at -30 °C). Atmospheric INP concentrations vary over several orders of magnitude at a single temperature and strongly increase as temperature approaches the homogeneous freezing threshold of water. To further quantify the INP concentration in nature and perform systematic laboratory studies to increase the understanding of the properties responsible for ice nucleation, a new drop freezing instrument, the DRoplet Ice Nuclei Counter Zurich (DRINCZ) is developed. The instrument is based on the design of previous drop freezing assays and uses a USB camera to automatically detect freezing in a 96-well tray cooled in an ethanol chilled bath with a user friendly and fully automated analysis procedure. Based on an in-depth characterization of DRINCZ, we develop a new method for quantifying and correcting temperature biases across drop freezing assays. DRINCZ is further validated performing NX-illite experiments, which compare well with the literature. The temperature uncertainty in DRINCZ was determined to be ± 0.9 ˚C. Furthermore, we demonstrate the applicability of DRINCZ by measuring and analyzing field collected snow samples during an evolving synoptic situation in the Austrian Alps. The field samples fall within previously observed ranges for cumulative INP concentrations and show a dependence on air mass origin and upstream precipitation amount.

1 Introduction

In the atmosphere, ice plays an important role in initiating precipitation and affects the radiative properties of clouds. As much as 80% of land falling precipitation initiates through the ice phase (Mülmenstädt et al., 2015), making it essential to understand the pathways for ice formation in the atmosphere. The ratio of cloud droplets to ice crystals in a mixed-phase cloud (MPC) alters the radiative properties of the cloud and its lifetime (Lohmann and Feichter, 2005; Matus and L'Ecuyer, 2017; Tan et al., 2016). This ratio is important for future climate projections as warmer temperatures will lead to a decrease in ice content, ultimately increasing cloud lifetime and cloud albedo (Tan et al., 2016). Additionally, ice formation at temperatures above -38 ˚C in the atmosphere occurs primarily in MPCs through the freezing of cloud droplets (Ansmann et al., 2009; Boer et al., 2011; Westbrook and Illingworth, 2011). Therefore, understanding ice formation in conditions associated with MPCs is of the utmost importance.

When an ice nucleating particle (INP) gets immersed in a cloud droplet~~s~~ either by acting as cloud condensation nucleus or through scavenging by a cloud droplet~~s~~, the INP can induce ice formation by reducing the energy barrier associated with the formation of an ice germ and thus freeze at warmer temperatures than homogeneous freezing (Vali et al., 2015). To reproduce the immersion freezing pathway in the laboratory, several methods are used. Single particle methods, such as continuous flow diffusion chambers (Rogers, 1988; Stetzer et al., 2008) operated at water supersaturated conditions (DeMott et al., 2015, 2017; Hiranuma et al., 2015), or with extended chambers that activate individual particles into cloud droplets before exposing them to supercooled conditions (Burkert-Kohn et al., 2017; Kohn et al., 2016; Lüönd et al., 2010) allow for the quantification of the number concentration of INPs as a function temperature. Larger laboratory based single particle methods for examining INPs in the immersion mode include expansion chambers where cloud droplets are first formed by adiabatic cooling due to the expansion of an air volume (Niemand et al., 2012) or experiments where droplets are initially activated and then subsequently cooled as they travel through a laminar flow tube (Hartmann et al., 2011). Aerosols introduced into such systems by dry dispersion or atomization of suspensions and solutions ~~thus~~ allow~~ing~~ for a range of particulates to be examined. However, the single particle methods have detection limitations due to the background ice crystal concentration of the chamber and the optical methods for discriminating between ice and water. Due to the rarity of INPs at MPC conditions, single particle methods are typically unable to quantify INP concentrations within natural ambient samples at temperatures higher than approximately -22 ˚C in remote regions ~~or~~ without the use of concentrators (Cziczo et al., 2017).

In contrast bulk methods such as, drop freezing assays (Hill et al., 2014; Stopelli et al., 2014; Vali, 1971), differential scanning calorimetry (Kaufmann et al., 2016; Pinti et al., 2012) and microfluidic devices (Reicher et al., 2018; Riechers et al., 2013; Stan et al., 2009; Tarn et al., 2018) immerse the samples in water and can be used to detect ~~even the lowest~~lower atmospheric INP concentrations. The majority of atmospheric INP concentrations at temperatures above -15 ˚C has been quantified using drop freezing assays. To retrieve the concentrations of INP from such bulk suspensions, Vali, (1971; 2019) showed that by

dividing a sample into several aliquots, it is possible to calculate the number of INPs present in the sample as a function of temperature. The probability for more than one INP in an aliquot that freezes at the same temperature can be predicted using Poisson's Law (Vali, 1971). Following Vali (1971), the cumulative number of INPs in a given sample for each temperature can be calculated as:

$$INP(T) = \frac{-ln(1-FF(T))}{V_a} \quad (1)$$

where $FF(T)$ is the fraction of frozen aliquots at a given temperature, T, and V_a is the volume of an aliquot. As can be seen in Eq. 1, the only way to extend the range of measureable INPs across temperature scales is to change V_a. Due to instrumental limitations, it is often difficult to change V_a by significantly enough values for a change in $INP(T)$ within a single instrumental setup. Rather it is easier to dilute the initial sample thereby reducing the number of INPs in each aliquot. Alternatively, to explore freezing towards warmer temperatures, field samples (e.g. rain or snow samples) can be concentrated by evaporating a part of the water. To account for dilution, Eq. 1 can be rewritten as:

$$INP(T) = \frac{-ln(1-FF(T))DF}{V_a} \quad (2)$$

where DF is the dilution factor of the initial sample. However, in some cases dilution alone cannot be used to observe the total number of $INP(T)$ due to the presence of impurities that act as INPs in the water used for dilution (Polen et al., 2018). Therefore, it is necessary to use different bulk techniques that measure aliquots with volumes that span several orders of magnitude, typically microliter to picoliter volumes (Harrison et al., 2018; Hill et al., 2014; Murray et al., 2010; Whale et al., 2015).

Studies have investigated the concentrations of INPs in the atmosphere over the last 50 years and show that the concentration in the atmosphere spans several orders of magnitude (Fletcher, 1962; Kanji et al., 2017; Petters and Wright, 2015; Welti et al., 2018). Some of the original studies investigated the INP concentrations in melted hail and snow samples e.g. (Vali, 1971). Since then, studies have diversified to sampling INPs directly from the air (Boose et al., 2016b; Creamean et al., 2013; DeMott et al., 2003; Lacher et al., 2017; Richardson et al., 2007; Welti et al., 2018), from precipitation (Christner et al., 2008; Hill et al., 2014; Petters and Wright, 2015; Stopelli et al., 2015) and investigated potential types of INPs in the laboratory from commercial and naturally occurring samples as well as field collected samples (Atkinson et al., 2013; Boose et al., 2016a; Broadley et al., 2012; Felgitsch et al., 2018; Hill et al., 2014; Hiranuma et al., 2015, 2019; Kaufmann et al., 2016; Murray et al., 2012; Pummer et al., 2012; Wex et al., 2015). Yet the atmospheric variability in INP concentrations remains unresolved (Hoose and Möhler, 2012; Kanji et al., 2017; Petters and Wright, 2015; Welti et al., 2018). In order to further quantify the variability of ambient INP concentration ~~responsible~~relevant for ice formation in MPCs and increase the ~~fundamental~~ understanding of the ice nucleation ability of laboratory and field collected samples~~–~~, we developed and characterized the DRoplet Ice Nuclei Counter Zurich (DRINCZ)~~,~~ DRINCZ is a drop freezing instrument to investigate ice nucleation at temperature conditions between -25 ˚C and 0 ˚C, representative for MPCs. Furthermore, DRINCZ complements and extends the INP concentration measurement capabilities of the single particle and bulk methods employed at ETH Zürich e.g. (Kohn

et al., 2016; Lacher et al., 2017; Lüönd et al., 2010; Marcolli et al., 2007; Stetzer et al., 2008). ~~Furthermore, t~~The automation of DRINCZ and its portable design allows for the acquisition of INP data in the field and laboratory, ultimately increasing the attainable information about the global distribution of INPs.

2 Instrument Design

DRINCZ is based on the design of Stopelli et al. (2014) and Hill et al. (2014), which was initially suggested by (Vali and Upper, 1995). It consists of a temperature controlled ethanol bath (Lauda ProLine RP 845, Lauda-Königshofen, Germany), a home-built LED light consisting of several LED light strips enclosed in an ethanol proof housing, a home-built 96-well tray holder and camera mount, a webcam (Microsoft Lifecam HD-3000) and a custom designed bath leveler, composed of a bath level sensor and valve (see Section 2.2) (Fig. 1a). The working principle is similar to that of Stopelli et al. (2014), in that a USB camera detects the light transmission through aliquots of sample. In DRINCZ, the aliquots are typically 50 µL and dispensed into a 96-well polypropylene tray (732-2386, VWR, USA). To avoid contamination, the top of the 96-well tray is sealed with a transparent non-permeable foil (Axgen, Platemax CyclerSeal Sealing Film, PCR-TS). The well tray is placed in the tray holder (Fig. A1) and left to rest for 1 min at 0 °C before the cooling ramp ~~experiment~~ is started. The webcam is programmed to take a picture every 15 seconds, which corresponds to a picture taken approximately every 0.25 ˚C decrease when the bath is cooled at a rate of 1 ˚C min^{-1}. Moreover, both the picture frequency and cooling rate are adjustable. Upon freezing, the light transmission through an individual well decreases (red circled well in Fig. 1b) due to the polycrystallinity of the ice frozen in the wells.

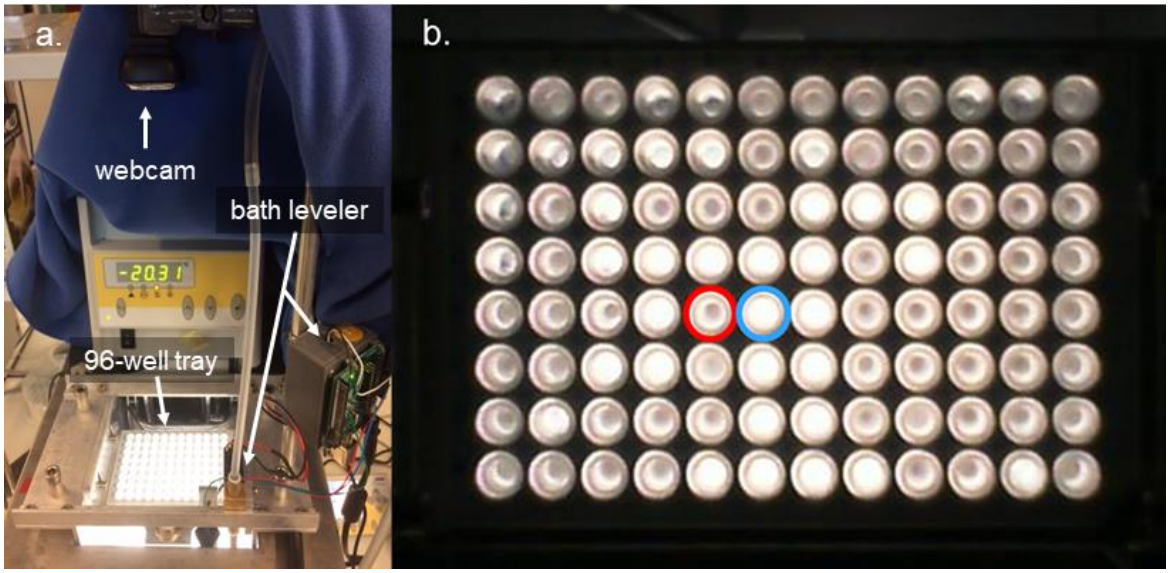

Figure 1: (a) Picture of DRINCZ. (b) Change in light transmission through the wells during an experiment with an example of an unfrozen (blue circle) and frozen (red circle) well.

The cooling cycle of the ethanol-based Lauda bath is controlled using LabVIEW® and the bath temperature is written to a text file that is then read in by MATLAB® during the analysis. In addition, MATLAB® is also used to take and save the pictures from the webcam. Both the LabVIEW® generated text file and pictures from the experiment are stored in the same folder for data handling. A suite of MATLAB® functions have been written to automatically analyze and store the data from each experiment, allowing for minimal user input (details of the code are provided in Appendix A) and rapid experiment throughput of approximately 30 minutes per experiment and 2 minutes to process the data for frozen fraction as a function of temperature.

2.1 Detection Method

Similar to Stopelli et al, (2014), ~~T~~the ice nucleation detection in DRINCZ is achieved by the attenuation of visible radiation due to a frozen well compared to transmission through a supercooled well. The images are analyzed by first detecting the pixels that correspond to each well of the 96-well tray and then calculating the change of the average well brightness during an experiment between one picture and the next. The well detection method is described in the following subsection, followed by the technique used to detect well freezing.

2.1.1 Circular Hough Transform for Well Detection

A fixed 96-well tray holder with an integrated webcam mount reduces variations in setting up the experiment. Nevertheless, small changes in the location of the webcam due to mechanical shock during transport or testing, can produce misidentified wells when algorithms rely on fixed well locations. Therefore, a freezing detection algorithm was developed to avoid errors arising from small changes in the location of the wells. To optimize contrast, the PCR tray holder was constructed out of aluminum so that light transmission only occurs through the wells (see Fig. A1). The high contrast between the illuminated wells and dark tray holder allows for the automatic detection of the wells using a Circular Hough Transform (CHT) (e.g. Atherton and Kerbyson, 1999). The CHT first identifies pixels along regions of ~~large brightness~~large gradients in brightness, to identify the pixels at the edge of the well. To determine the center of each well, the algorithm draws circles of varying diameter (ranging between 7 and 15 pixels in radius, which corresponds to the previously observed diameters of a well in terms of pixel number) ~~all centered~~ around these edge ~~edge of the~~ pixels and classifies the pixel intersecting the largest number of circles as the well center. The radius of the well is then given as the radius of the circles that led to the highest number of intersections. The pixels within a well are then identified as the ones encompassed by a circle drawn from a well center with the calculated radius as denoted by the red circles in Fig. 2a. Since the CHT identifies the well center locations in random order, they must be sorted based on their x and y coordinates using a pixel scale for spatial biases or refreezing results to be analyzed. The wells are sorted based on their center locations using the following equation:

$$C_i = \frac{y_i}{D} L_x + x_i \quad (3)$$

where C_i is the value of the well center based on its pixel location in y and x coordinates, y_i and x_i, respectively, with the origin taken as the pixel in the upper left hand corner of the image. L_x is the pixel number across the well array in the x

coordinate and D is the diameter (pixel number) of the wells. All the C_i values are then sorted to ensure that the wells are identified based on their location independent of the experiment.

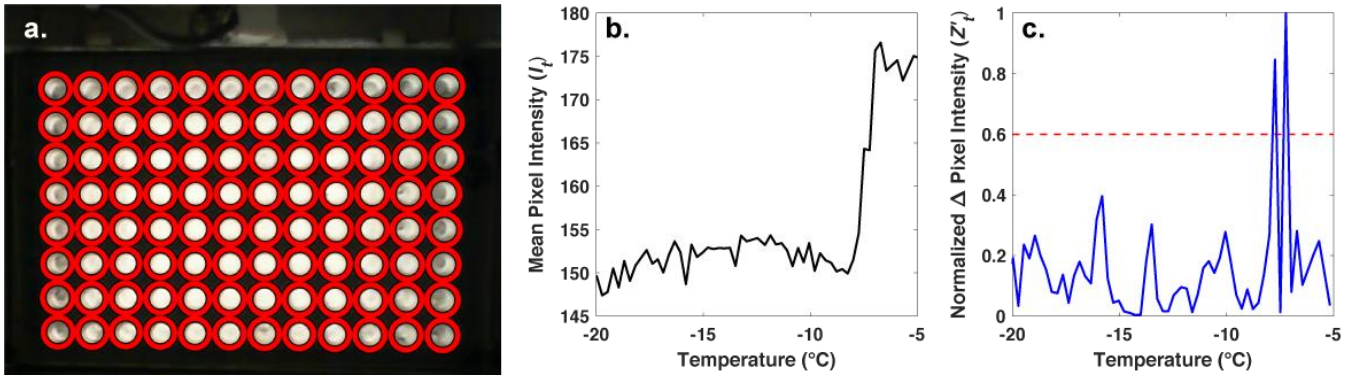

Figure 2: (a) Automatic detection of the wells (red circles) using a CHT. (b) Light intensity or I_t of a single well as a function of temperature as observed by the webcam and (c) the normalized change in pixel intensity, Z'_t, for the same well as in b between subsequent pictures taken during an experiment, as a function of temperature. The most intense peak ~~right hand peak~~ corresponds to the ~~is the~~ ice nucleation temperature and the second most intense peak ~~initial freezing and the second peak~~ is due to the slow freezing of the solution after nucleation. The dashed red line represents the 0.6 threshold required for a well to be classified as frozen.

2.1.2 Freezing Detection

With the well locations identified, the intensity values of the pixels within each well are averaged for each image recorded during an experiment (I_t). The change in I_t between subsequent images is used to identify the image where freezing occurred and the corresponding temperature (Fig. 2b). However, due to the slow freezing process which is limited by the latent heat release, the light transmission of a well continuously changes until the water is completely frozen as can be seen as two large peaks in Fig. 2c. To correctly identify the point in time when ice nucleation and not just freezing within the well occurs, the maximum change in I_t between subsequent images is normalized to 1 using the following procedure:

First, the Z-score (Z_t) of I_t is taken to level out differences in illumination within the 96-well tray:

$$Z_t = \frac{I_t - \mu}{\sigma} \quad (4)$$

where μ and σ are the mean and standard deviation of I_t for all ~~recorded~~ images of a well, respectively. The absolute value of the time derivative or the change in Z_t between subsequent images (dt) is given as:

$$Z'_t = \left|\frac{Z_t}{dt}\right| \quad (5)$$

Z'_t is then normalized to 1 by dividing by the maximum Z'_t of the well. The normalization ensures that a fixed threshold for the identification of ice nucleation can be used rather than relying on a fixed change in light transmission through the well as done by other drop freezing setups (Beall et al., 2017)~~.~~. This ensures that the initial freezing detection is independent of the absolute change in light transmission through a well ~~during initial freezing~~. Based on validation experiments, a threshold value of 0.6

$\left(\frac{z_t'}{\max(z_t')} \geq 0.6\right)$ was found to be best for detecting the initial freezing and to avoid assigning subsequent changes in transparency as a nucleation event due to slow freezing.

2.2 Bath Leveler

Due to the thermal contraction of the ethanol in the chilled bath between 0 and -30 ˚C, the ethanol level within the bath decreases during an experiment, affecting the immersion level of the wells and thus the thermal contact. It has been shown that large vertical gradients of up to 1.8 °C can exist between the bottom of a well and the air above it in block-based drop freezing setups (Beall et al., 2017). We anticipate vertical gradients to be reduced in DRINCZ due to the direct contact between the cooling medium (ethanol) and the well tray. Therefore, we incorporated a bath leveler composed of a ~~To keep the ethanol level constant, a~~ level sensor and solenoid valve ~~are incorporated into the setup~~to ensure that the ethanol level remains constant. The level sensor (Honeywell LLE 102101 liquid level sensor) detects when the ethanol falls below a fixed level relative to the wells and triggers the solenoid valve (Kuhnke 64.025, 12 VDC valve) to open, allowing additional ethanol to flow into the bath. The level sensor and solenoid are monitored and controlled using a 'sketch' written in Arduino (Arduino Uno Rev3 SMD). In order to minimize ~~a possible~~ thermal gradients by adding warm ethanol to the bath, the ethanol is precooled to 0 ˚C using an ice water bath and then added through a copper pipe that extends to the bottom of the bath. Thus, the bath leveler ensures that the wells remain in good thermal contact due to a constant level of ethanol during experiments, while minimizing ~~potential~~ temperature fluctuations within the bath. The resulting increased reproducibility of experiments due to the bath leveler is discussed in section 3.4.

3 Validation

The validation of the instrument is presented in four sections, with the first discussing the temperature calibration followed by discussing the observed bias in freezing, the quantification of instrumental uncertainty and lastly, the improved reproducibility of DRINCZ due to the addition of the bath leveller.

3.1 Temperature Calibration

The temperature reported as the freezing temperature is based on the ethanol bath temperature measured by the Lauda chiller (T_{lauda}). In order to correct for the difference between the temperatures of the sample in the wells (T_{well}) and T_{lauda}, a temperature calibration was performed. The calibration was conducted by measuring the temperature (Type K thermocouple) within the four corner wells and a center well of the 96-well tray (Fig. 3a). The same thermocouple was used for all the well temperature measurements to avoid biases between different thermocouples. The wells were filled with 50 µL of ethanol instead of water to extend the calibration across the entire experimental temperature range of DRINCZ without the interference of freezing. The temperature bias between the wells and T_{lauda} was measured every 1 ˚C while the bath was cooled at the typical ramp rate

of 1 ˚C min^{-1}. The calibration was performed three times for each well (Fig 3b). Not surprisingly, we found that the ethanol temperature in the bath was consistently lower than the temperature in the five calibration wells and the difference between bath and well temperature increased linearly as the bath temperature decreased. Based on these results the linear function $T_{corr} = 0.917 * T_{lauda} + 1.3$, with T_{lauda} in ˚C (black line in Fig. 3b) was derived to correct the well temperature. The maximum standard deviation ~~is in~~taken as the temperature difference between the temperature fit and the individual well temperature ~~and~~ was ~~with a maximum standard deviation of~~ ±0.6 ˚C.

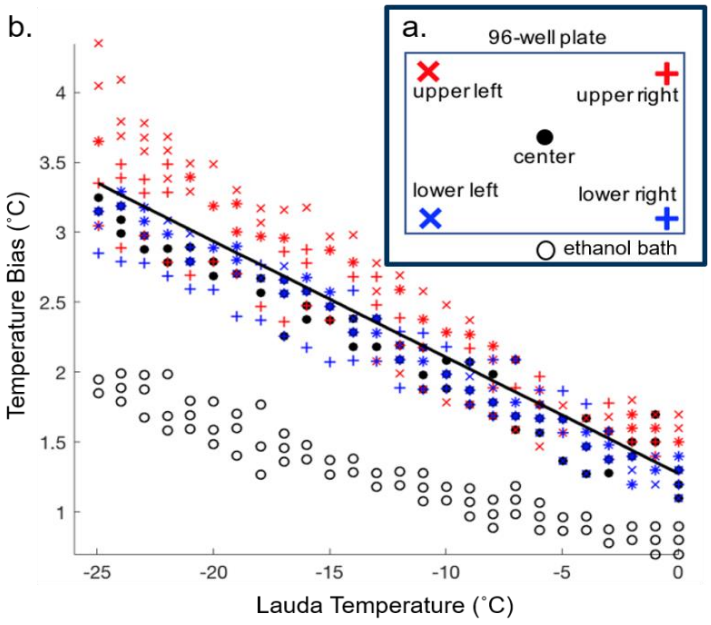

Figure 3: (a) Locations of the type-K thermocouples tested during the temperature calibration. Additionally, the temperature difference between the Lauda temperature and the ethanol bath was measured at the indicated location (black open circle). (b) The temperature bias between the wells and ethanol bath is displayed versus the Lauda bath temperature. The linear temperature correction is shown in black.

3.2 Freezing Bias across the 96-well Tray

The temperature calibration discussed above revealed potential variations in the well temperatures between the corner and the center wells. We thus quantified the bias for individual wells, but conclude that it is within the instrument experimental error as discussed below. To do so, 20 pure water (Molecular Biology Reagent, W4502 SigmaAldrich; hereafter referred to as SA water) experiments were analyzed. SA water was chosen for this analysis due to its homogeneity and low freezing temperature, where the observed spread in well temperature was maximized (see Fig. 3). For each well the median freezing temperature (or temperature when frozen fraction (FF) = ~~50 %~~0.5) ($\widetilde{w}_i$) was compared to the median freezing temperature of the 4 corner wells ($\widetilde{w}_{4ref}$) used for the temperature calibration (see Fig. 3a and Fig. A2 for the distribution in freezing temperatures of the wells). The difference between $\widetilde{w}_{4ref}$ and $\widetilde{w}_i$ ($\widetilde{w}_{4ref} - \widetilde{w}_i$) is shown in Fig. 4a. The red (blue) shading indicates a warm (cold) bias

and signifies that the solution in these wells are exposed to warmer (colder) temperatures than the average of the four reference wells. The higher concentration of red shades in the middle of the tray suggests that the center of the tray is exposed to as much as 1.5 ˚C warmer ethanol flow than the tray periphery. Indeed, the chilled ethanol circulates clockwise in the Lauda chiller and thus the freezing appears to track the flow (arrows in Fig. 4). Thus, the ethanol circulation explains the observed bias in freezing temperatures across the well plate. The same analysis procedure was applied to the same 20 samples separated by user (12 and 8 experiments) and a similar bias was observed (see Appendix Fig. A23). Therefore, the reported bias is instrumental, reproducible and any potential user bias can be excluded. The bias was found to be statistically significant at the 95% confidence interval for 30% of the wells and resulted in an overall bias of 0.23 ˚C (see Fig 4b and Appendix A). As such, a well by well bias correction was developed and tested as described in Appendix A. Although the bias correction performed as expected, the bias of 0.23 ˚C falls within the instrumental uncertainty as discussed in Section 3.3 and is therefore not applied to DRINCZ measurements by default. Nevertheless, the potential benefits and impacts of a bias correction is discussed in the following section.

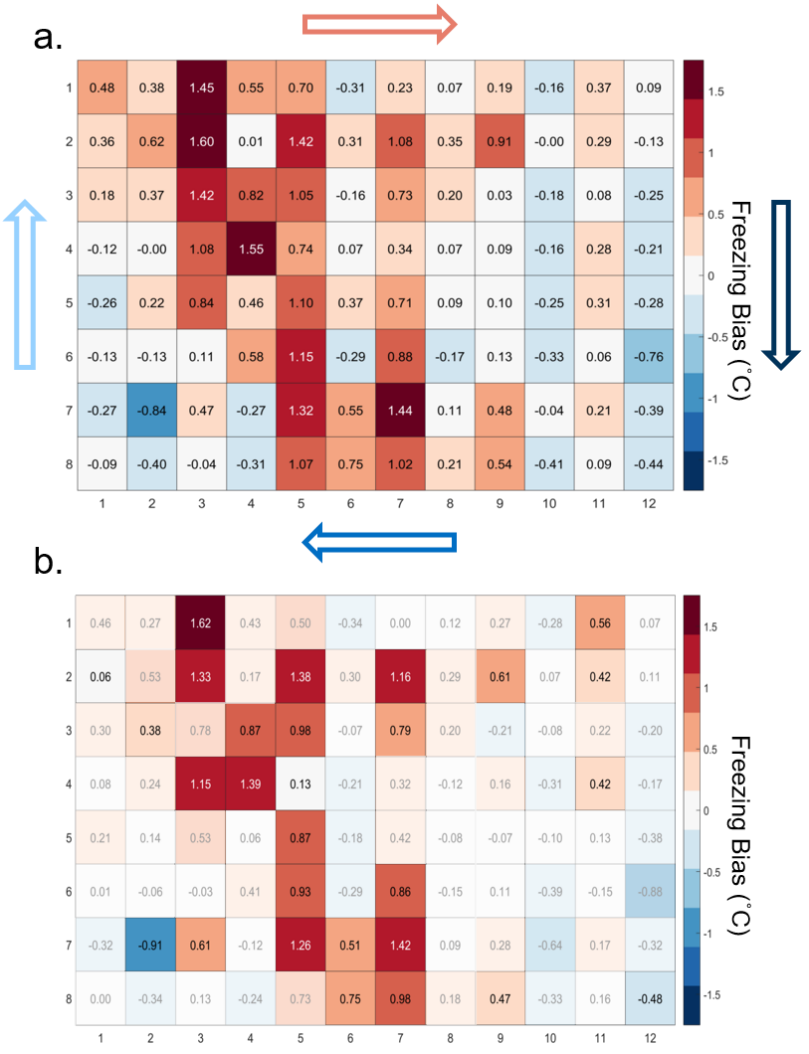

Figure 4: (a) Bias in the freezing of SA water ($\tilde{w}_{4ref} - \tilde{w}_i$ in ˚C) based on the median value of each well over 20 experiments relative to the median temperature of freezing for the 4 corner wells used during the temperature calibration. A positive (negative) bias indicates that the wells experience a warmer (colder) temperature than the four corner wells used for temperature calibration and therefore freeze at lower (higher) temperatures than reported. The arrows represent the ethanol circulation in the chiller and the color represents the temperature trend of the ethanol as it circulates in the bath with dark blue being the coldest and red the warmest. (b) Mean freezing bias of SA water between the four reference wells and each well ($\bar{w}_{4ref} - \bar{w}_i$). Positive (negative) values indicate, as denoted by shades of red (blue), wells that systematically freeze at colder (warmer) temperatures and therefore experience warmer (colder) temperatures than reported. Statistically insignificant biases as determined by a Welch's *t*-test (see Eq. A1) are depicted as greyed out.

3.2.12 Impact of Bias Correction on Frozen Fraction

By accounting for the bias in freezing temperature across the 96-well tray by first applying the temperature calibration and then the bias correction such that corrected well value ($\bar{\bar{w}}_i$) becomes:

$$\bar{\bar{w}}_i = \bar{w}_i + (\bar{w}_{4ref} - \bar{w}_i), \quad (6)$$

the slope of the *FF* curves steepens and becomes smoother, which is expected as the observed freezing temperatures become more constrained (see Fig. 5). Although the median freezing temperature with and without the bias correction only changes by 0.2 ˚C (consistent with the correction of the mean bias of 0.23 ˚C found above), the narrowing of the freezing temperature distribution is significant at the 95% significance level (Welch's *t*-test, see Eq. A1). This result shows that by using the spatial dependent freezing information of a well from optically based drop freezing instruments like DRINCZ, temperature can be better constrained. Such a bias correction should also be applicable to freezing methods that use block based cooling, where gradients across the block ~~may exist~~have been observed or modelled (Beall et al., 2017; Harrison et al., 2018).

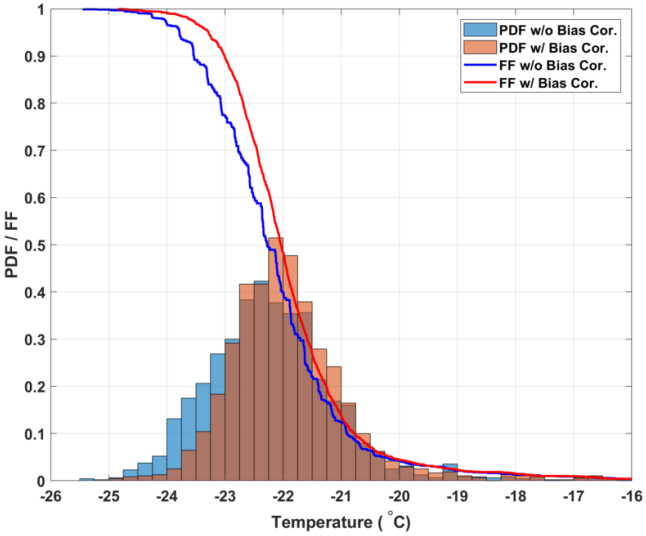

Figure 5: Histograms representing the probability distribution functions for freezing temperatures of the 20 SA water experiments without (blue bars) and with the bias correction (red bars). The calculated cumulative distribution functions, or frozen fraction curves without and with the bias correction are represented as the blue and red lines, respectively.

3.3 Instrument Uncertainty

The instrumental uncertainty for DRINCZ is assessed by using the standard deviation in the observed freezing temperatures of the SA water experiments across all wells in combination with the error in the temperature of the wells established during the temperature calibration. The standard deviation of the freezing temperature of the SA water is dependent on *FF*, with a minimum at ~~50%~~0.5 *FF* (Fig. 6a). This dependence is expected as the ~~50%~~0.5 *FF* corresponds to the most likely temperature for the SA water to freeze and therefore, should show the least variability across the 20 experiments used in the analysis. Furthermore, by using the 0.5 *FF* the influence of contamination and outliers is minimized. The standard deviation at each *FF* is the uncertainty due to the instrument as well as the variability in the freezing temperature of the SA water and represents the upper limit of the instrumental uncertainty. Given the contribution to the uncertainty due to the variability of the freezing temperature of the SA water, the standard deviation at *FF* = ~~50 %~~0.5 can be used as the upper limit of the instrumental uncertainty across the entire *FF* range. Incorporating a bias correction results in a negligible average difference in the standard

deviation (as shown by dashed lines in Fig. 6a). Thus, the upper limit of the instrumental precision is ± 0.3 ˚C (the mean of the standard deviation of freezing temperature over the entire freezing spectrum).

Although the instrumental precision indicates that DRINCZ is very reproducible (± 0.3 ˚C), the accuracy in the reported temperature must be accounted for. Based on the temperature calibration, the standard deviation of the well temperatures is temperature dependent. At the coldest temperatures of the freezing range of the SA water (~ -25 ˚C), the standard deviation of the well temperatures is largest, likely due to the increased gradient between the bath and air temperature and therefore, the importance of the ethanol circulation through the bath is increased. To account for this temperature dependence, the maximum standard deviation of ± 0.6 ˚C from the temperature calibration, corresponding to the lowest observable freezing temperature in DRINCZ (freezing temperature of SA water) is used. Therefore, when accounting for both the precision of the measurements and the accuracy of the temperature, the overall uncertainty of the reported freezing temperature of a well in DRINCZ is ± 0.9 ˚C. This value is comparable to other recently developed drop freezing techniques, which report uncertainties ranging between ± 0.9 ˚C (Harrison et al., 2018) and ± 2.2 ˚C (Beall et al., 2017).

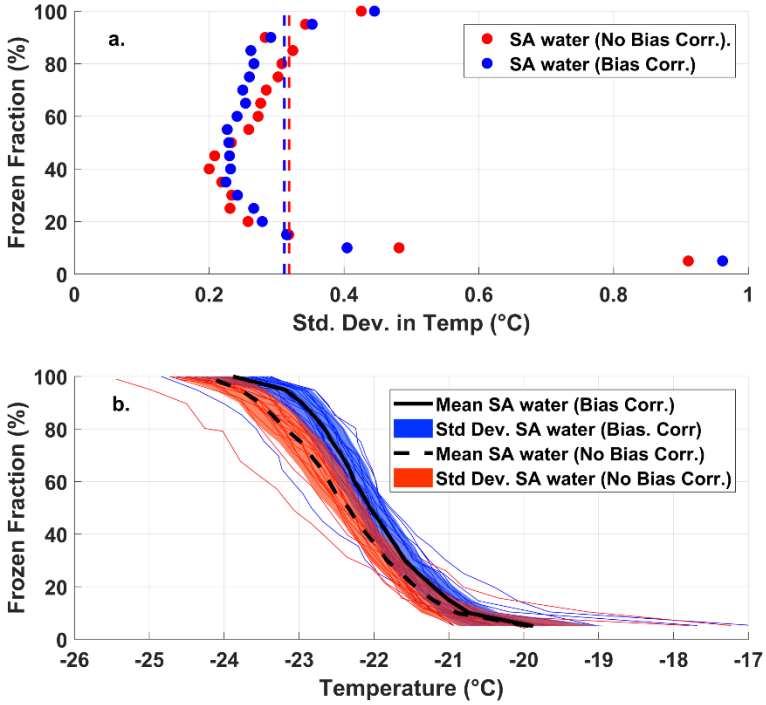

Figure 6: (a) *FF* and the corresponding standard deviation of the freezing temperatures from the 20 SA experiments with and without the bias correction shown as blue and red dots, respectively. The red and blue dashed lines represent the standard deviations in temperature averaged over all *FF* values without and with the bias correction, respectively. (b)The *FF* of the 20 SA water experiments as a function of temperature with and without the bias correction (thin blue and red lines, respectively). The color fill represents the standard deviations of the SA water from the mean freezing temperature with (solid black line) and without (the dashed black line) the bias correction.

3.4 Importance of the Bath Leveler

To assess the impact of the decreasing ethanol level on experiments in DRINCZ, 32 experiments with SA water without a bath leveler were compared to the 20 SA water with a bath level sensor, the same 20 SA water discussed in the previous section. Figure 7a shows that the bath sensor reduces the spread in freezing temperatures observed. The decrease in the ~~50 %~~0.5 *FF* temperature without the bath leveler is due to a larger gradient between the aliquot and the bath temperatures, thus the well is warmer than expected, requiring further cooling to observe freezing. The additional cooling in combination with the variable starting level of the ethanol relative to the wells in the cases of no bath leveler is responsible for the longer freezing tail of the *FF* curve (blue line) at higher *FF*s. Without the bath leveler, the initial height of ethanol relative to the wells is user dependent and not reproducible, leading to both the higher and lower observed freezing temperatures.

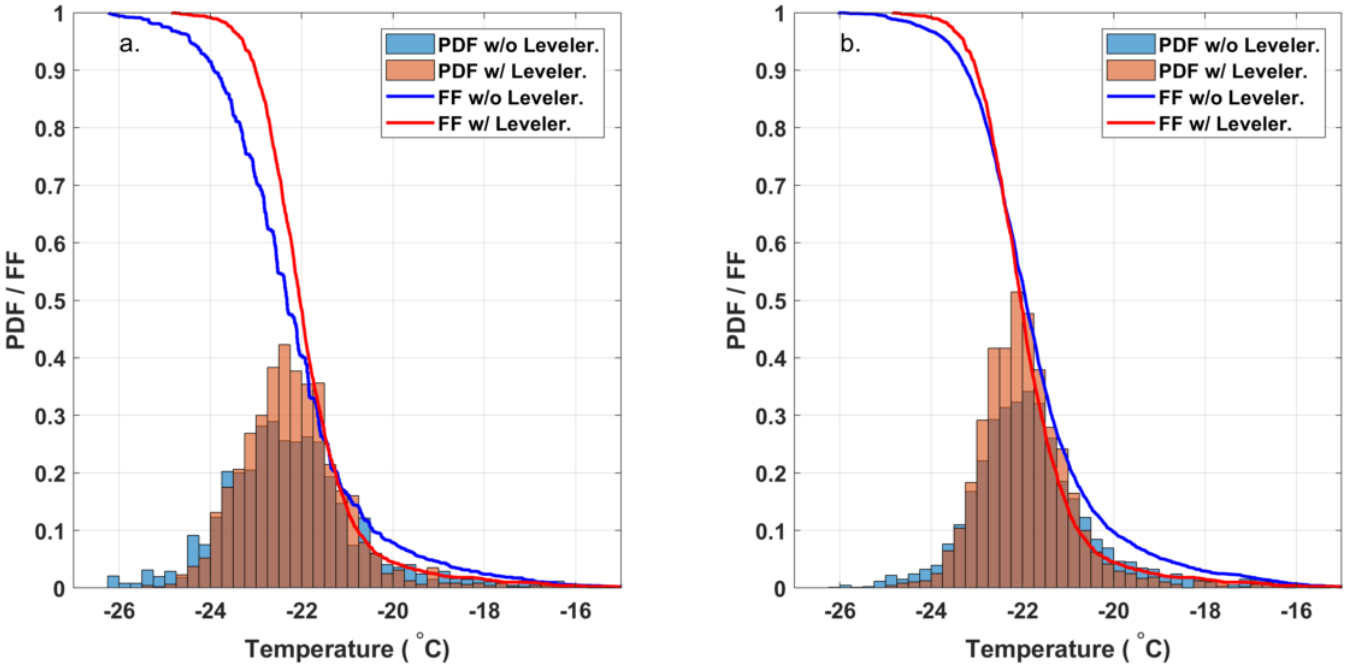

Figure 7: (a) Comparison of the freezing temperature of SA water without (32 experiments, blue) and with (20 experiments, red) the bath leveler. The histograms are normalized to represent the PDF of the freezing temperatures and the lines represent the mean FF curves of the SA water experiments. (b) Shows the same as panel a, except that a bias correction is applied to both sets of experiments.

Although the median freezing temperature (*FF*=~~50 %~~0.5) only decreased by 0.25 ˚C without the bath leveler, the freezing curves steepen when the bath leveler is incorporated in DRINCZ, leading to a decrease of the standard deviation from ± 1.4 to ± 1.0 ˚C over the entire *FF* range. A bias correction applied following the procedure in Section 3.2 reduces the issues associated with a variable bath level as seen by the similar *FF* curves and histograms normalized using the probability density function (PDF) estimate in Fig. 7b for experiments with and without the bath leveler. The difference in mean freezing temperatures decrease to 0.05 ˚C at *FF*=~~50 %~~0.5 and the standard deviation of the SA water freezing temperature without the leveler

decreases from ± 1.4 to ± 1.2 ˚C over the entire *FF* range. This decrease is expected as the bias correction is designed to reduce the spread in freezing temperatures within the 96 aliquots. Although the bias correction reduces the need for a bath leveler in DRINCZ, the bias is instrument dependent and may be less pronounced in other drop freezing setups. Therefore, we recommend the use of a bath leveler in any bath-based drop freezing devices.

4 Freezing Experiments

To verify the performance of DRINCZ in the context of other published drop freezing techniques, we use the SA water experiments to characterize the instrumental background (Section 4.1) and perform freezing experiments with NX-illite suspensions (Section 4.2). To demonstrate applicability of the instrument to analysis of field samples, the evolution of the ice nucleating ability of atmospheric aerosol particles collected in snow samples at the Sonnblick Observatory in the Hohe Tauern region of Austria during a mid-latitude storm system is assessed in Section 4.3. Lastly, some uncertainties associated with measuring INP in snow samples (Section 4.4) and further validation of DRINCZ through dilutions are discussed (Section 4.5).

4.1 Background of DRINCZ

The background freezing due to the experimental technique and the SA water used to suspend and dilute samples must be known to discriminate freezing events due to the sample from freezing events due to the water used. Furthermore, an SA water sample is run as a standard at the beginning of each measurement day to ensure the system is operating correctly. The 20 SA water experiments are therefore used to assess the instrument background freezing. It is important to note that in cases where solvents other than SA water are used or where contamination from a sampling technique (e.g. snow collection or impinger measurements) is possible, a different background calculation must be used to accurately assess the freezing ability of a sample. The background of DRINCZ when used with SA water, is calculated by fitting the 20 SA water experiments with a five parameter Boltzmann fit. The five parameter version was chosen to account for asymmetry (Spiess et al., 2008) in the freezing of the SA water but due to the minimum and maximum values of *FF* given as 0 and 1, respectively, the fit reduces to three parameters and takes the form:

$$FF_{BGfit}\left(T_{frzBG}, a, b, c\right) = \frac{1}{\left(1+e^{a\left(T_{frzBG}-b\right)}\right)^{c}}, \quad (8)$$

where FF_{BGfit} is the fitted *FF* of the SA water as a function of the observed freezing temperatures of the SA water, T_{frzBG}, and the fitting parameters, a, b, c represent the slope of the fit (a = 1.9651), the inflection point (b = -22.7134) and the asymmetry factor (c = 0.6160), respectively. The value of 1 in the numerator represents the maximum *FF*. The fit and associated coefficients (including 95% confidence range and r^2) are shown in Table 1 and Fig. 8 respectively.

Table 1: Coefficients for the three parameter Boltzmann fit of the SA water freezing background and 95th percentile confidence interval bound values.

	a	b	c	r^2
Best	1.9651	-22.7134	0.6160	0.97
-95th %	1.7254	-22.8955	0.4683	N/A
+95th %	2.2049	-22.5312	0.7637	N/A

The fitted freezing background is used to correct for the contribution of SA water to the observed freezing of a sample. To account for the presence of multiple ice nucleating particles coexisting in a single well, the background is removed by subtracting the differential nucleus concentration of the background from that of the sample (Vali, 1971, 2019). The differential nucleus concentration ($k(T)$) is initially defined in Vali (1971) as:

$$k(T) = -\frac{1}{V_a \Delta T} \cdot ln\left(1 - \frac{\Delta N}{N(T)}\right), \quad (9)$$

where $N(T)$ is the number of unfrozen aliquots at the beginning of a temperature step while ΔN is the number of aliquots that freeze during the temperature step (between pictures) or ΔT.

The background corrected differential nucleus concentration ($k_{corr}(T)$) is obtained by:

$$k_{corr}(T) = k_{sam}(T) - k_{bg}(T), \quad (10)$$

where $k_{sam}(T)$ and $k_{bg}(T)$ are the sample and background differential nucleus concentration, respectively. The background corrected $FF_{cor}(T)$ is then achieved by inverting Eq. 9 and taking the cumulative sum of $k_{corr}(T)$:

$$FF_{cor}(T) = 1 - exp(-\sum[k_{corr}(T) \cdot \Delta T] \cdot V_a), \quad (11)$$

An example of the impact of the background correction on the *FF* of the diluted snow sample collected on Nov 30th 2017 (discussed in section 4.3) is shown in Fig. 8.

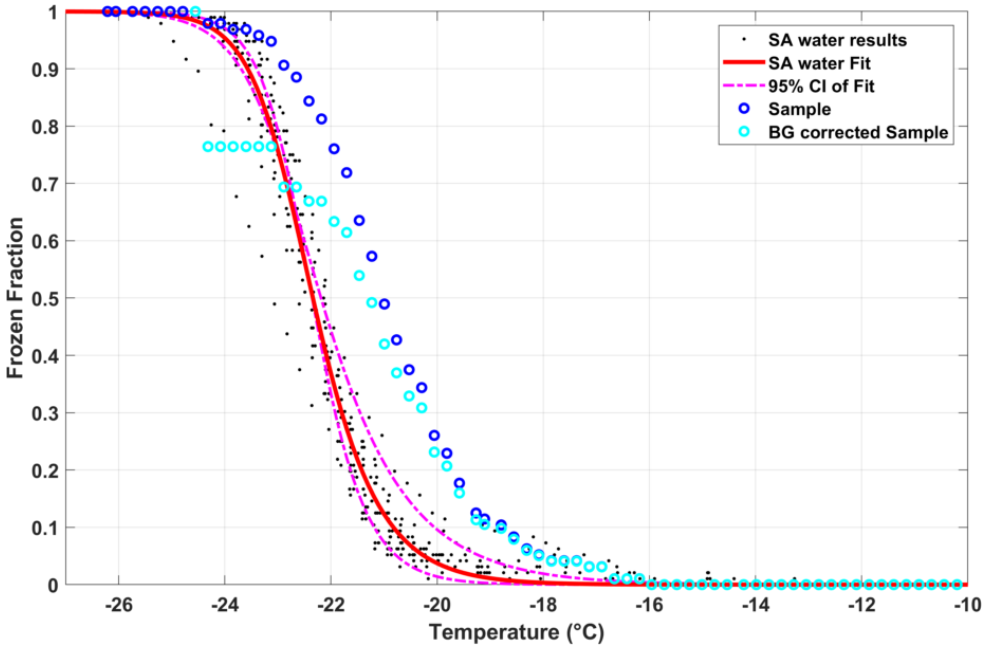

Figure 8: SA water data (black dots) and corresponding fit (red line, Eq. 8) including the 95th percentile confidence interval (dashed-dot magenta lines). The blue circles represents the diluted snow sample collected on Nov 30th 2017 which is then corrected for the contributions of freezing from the SA water using the background correction ($FF_{cor}(T)$ as described in Eq. 11; cyan circles).

4.2 Comparison of DRINCZ to other immersion freezing techniques

To validate the performance of DRINCZ, we use different wt. % NX-illite suspensions to compare the results from DRINCZ to those summarized in Hiranuma et al. (2015), Beall et al. (2017) and Harrison et al. (2018). In the atmosphere, illite constitutes up to ~40 % of the transported dust fraction (Broadley et al., 2012; Murray et al., 2012), making it an excellent surrogate for atmospherically relevant dust. An initial stock suspension of 0.1 wt. % NX-illite was prepared with SA water and then diluted to produce mass concentrations of NX-illite of 0.05 and 0.01 wt. %. The suspensions were manually shaken for 30 s, poured into a dispensing tray and then immediately pipetted into the well plate. Triplicates of each suspension concentration were ~~Three mass concentrations of NX-illite (0.01, 0.05, and 0.1 wt. %) were~~ investigated with DRINCZ (see Fig. A4 for *FF* curves) and then normalized to the number of active sites per BET-derived surface area (n_{sBET}) using a variation of Eq. 2 as follows:

$$n_{sBET} = -\frac{\ln(1-FF)}{V_a * SA_{BET} * C_{NX}}, \quad (12)$$

where SA_{BET} is the BET surface area of the particles used (NX-illite) and C_{NX} is the mass concentration of NX-illite in an experiment.

The n_{sBET} of NX-illite calculated using Eq. 12 from the measurements made with DRINCZ and background corrected (using Eq. 11) falls within the results from Hiranuma et al. (2015), Beall et al. (2017) and Harrison et al. (2018) (Fig. 9). In theory,

n_{sBET} should be insensitive to concentration as the number of ice nucleating sites is normalized to the total surface area. Indeed, the differing weight percent samples overlap to an extent (Fig. 9). Furthermore, the lower-weight-percentage samples extend the observable n_{sBET} to higher values and colder temperatures~~, as expected~~. Similar to the observations of Harrison et al. (2018), ~~a few of the~~the data points from the 0.01 wt. % ~~solution~~ suspension appear as outliers at the warmest temperatures. However, it is not possible to determine if these outliers are due to random freezing events that occur at high temperatures and therefore produce elevated cumulative n_{sBET} values at lower temperatures or ~~This is likely~~ if they are due to an uneven distribution of the active sites in each aliquot ~~and~~ that may ~~be the~~ result from~~of~~ diluting a single stock ~~solution~~ suspension rather than ~~producing~~ preparing individual weight percent ~~solutions~~ suspensions (Harrison et al., 2018). Thus a spread equivalent to or less than the spread in the concentrations, up to an order of magnitude in this case, can be expected. Furthermore, ~~when accounting for~~considering the ± 0.9 ˚C uncertainty, depicted by the horizontal error bars, the ~~results~~ differences between concentrations ~~become more similar~~are not significant. They~~and~~ fall within the same range as the measurements of Beall et al.~~,~~ (2017~~) who used similar concentrations of NX-illite~~ and between BINARY and Leeds-NIPI and IR-NIPI at colder temperatures (Fig. 9). The overlap between the n_{sBET} measured with DRINCZ and the NX-illite parameterization (Hiranuma et al., 2015) indicate that DRINCZ is capable of accurately measuring the concentration of INPs and their active sites in the immersion freezing mode (Fig. 9).

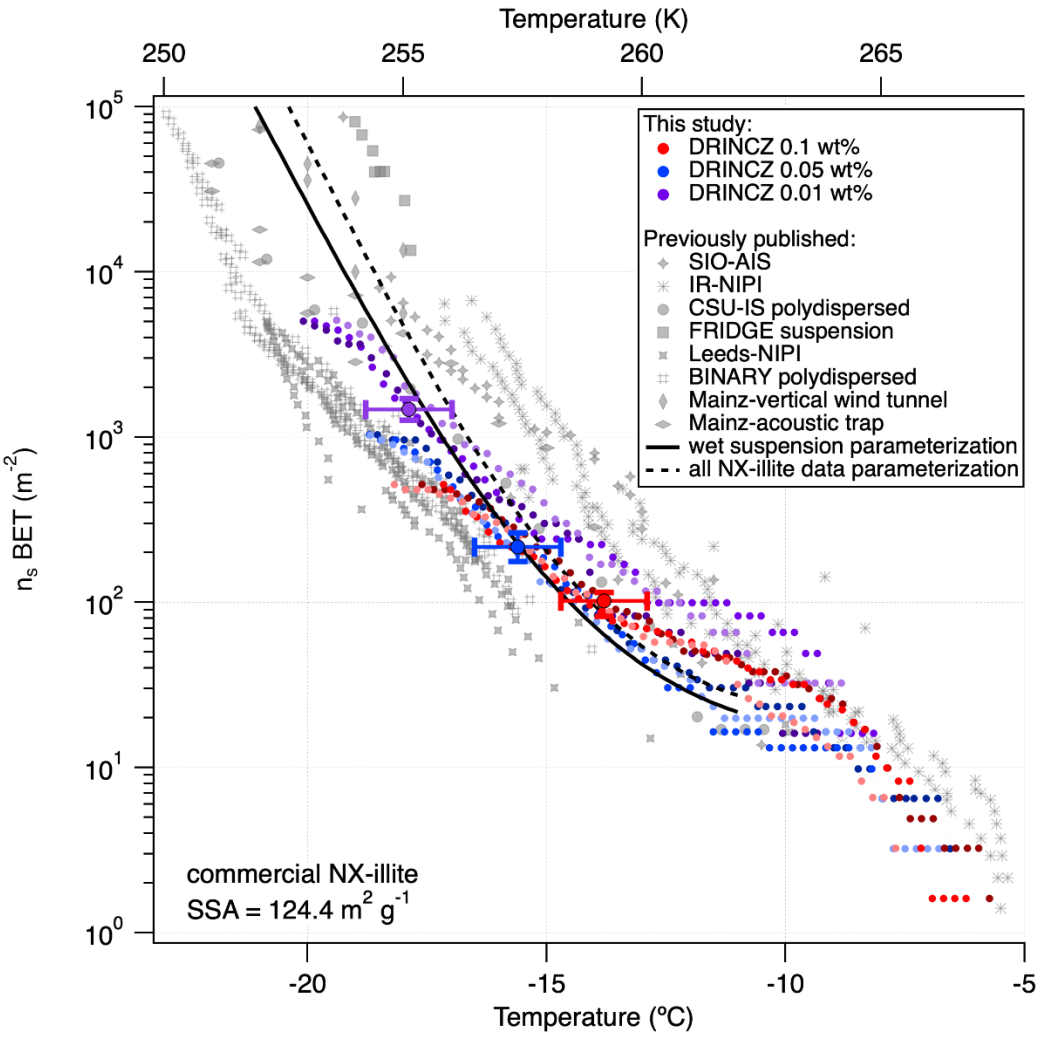

Figure 9: Triplicates of n_{sBET} (depicted by shading of the same color) ~~of~~ as a function of temperature for **three concentrations of NX-illite, 10^{-3} g ml^{-1} (red dots), $5x10^{-4}$ g ml^{-1} (blue dots) and 10^{-4} g ml^{-1} (purple dots),** ~~are measured as triplicates~~ measured **by DRINCZ** ~~and reported as a function of temperature~~**. An example of the temperature uncertainty and the uncertainty due to the background correction are depicted for each weight percent as horizontal and vertical error bars, respectively. Literature values from Hiranuma et al, (2015), Beall et al, (2017) and Harrison et al, (2018) are shown for comparison. n_{sBET} was calculated using a BET surface area of 124.4 m^2g^{-1} (Hiranuma et al., 2015).**

4.3 Ice Nucleating Particle Concentrations in Snow Samples from a Mountaintop Observatory in Austria

In order to demonstrate the performance of DRINCZ, snow samples collected between the 27th and 30th of November 2017 at the Sonnblick Observatory (SBO) were analyzed. The SBO is located at 3106 m on the summit of Mt. Sonnblick in the Hohe Tauern Region of Austria and has previously been used for cloud microphysical measurements (e.g. Beck et al., 2018; Puxbaum and Tscherwenka, 1998). Freshly fallen snow was collected from a wind-sheltered area where the snow could not

drift. A stainless steel shovel (Roth) was conditioned with snow by turning (10 times) in the surface snow next to the sampling site prior to sampling. The snow was then sampled into sterile NascoWhirlPaks (Roth) and then melted at room temperature (20 ˚C), immediately after which aliquots of snow-meltwater were filled into sterile centrifugation tubes (15 ml, Falcon tubes) and stored at -20 ˚C. The samples were ~~-~~shipped and stored frozen until processed with DRINCZ at the Atmospheric Physics ~~ETH Zurich -~~Laboratory at ETH Zurich, to ~~avoid~~ minimize any bacterial growth or changes due to liquid storage (Stopelli et al., 2014). The snowfall collected at SBO occurred during two snowfall events. The first event began on the 25th and ended overnight on the 26th (early hours of the 27th) while the second event (28th -30th) was associated with an intensifying upper level trough, a developing surface cyclone, a strong cold front and an associated secondary low (see Fig. A5 and A6).

The frozen fractions of five different snow samples were determined using DRINCZ and the cumulative concentration of active sites (or *INP(T)*, see Eq. 1) were normalized to per L of meltwater (n_{mw}) (Fig. 10). Overall, the n_{mw} of the snow samples fall within the range of previously reported values for precipitation samples (Petters and Wright, 2015) except for the November 30th sample. Within these samples, we identify (1) a particularly active snow sample (Nov 28th), (2) samples having intermediate IN activity (Nov 27, 29), and (3) a least active sample (Nov 30th). We attempt to compare these snow samples based on their air mass origin.

The snowfall sampled on the 28th had the highest n_{mw} of all collected samples (Fig. 10). The meteorological conditions and a comparison of back trajectories indicate that the air mass was associated with the warm sector of a synoptic system (Fig. A7) that originated from North America and the North Atlantic that then crossed France and Switzerland, before arriving at SBO (Fig. A8). In contrast, the arctic air mass responsible for the snowfall sampled on the 27th originated over Svalbard before crossing Iceland, the British Isles, Northern France and Germany (Fig. A8).

Even though the local conditions at SBO did not change significantly between the 28th and 29th, a decrease in n_{mw} was observed relative to the 28th and n_{mw} gradually decreased between the first and second sample on the 29th (Fig. 10). The back trajectories show that the origin of the air mass changed from North America and the North Atlantic on the 28th to exclusively originating over the North Atlantic on the 29th (Fig. A8). Additionally some of the back trajectories on the 29th show an increased interaction with the boundary layer over Europe (Fig. A8). Nevertheless, the decrease in n_{mw} suggests that if boundary layer aerosols from parts of Europe did reach the precipitating clouds at the SBO, they are less efficient INPs than the marine aerosols (Lacher et al., 2017, 2018) associated with the samples on the 27th and 28th.

Finally, the lowest n_{mw} observed were from meltwater collected on the 30th. The cold frontal passage and associated cold air advection caused the temperature to drop by 6 ˚C by noon on the 30th (Fig. A7) and the n_{mw} in the associated snowfall decreased substantially, exceeding the lower limit of previously reported n_{mw} values (Petters and Wright, 2015, Fig. 10). The decrease in n_{mw}, however, cannot be explained solely on the origin of the air mass as the arctic air mass on the 27th also crossed similar

parts of the UK or had significant interaction with the marine boundary layer. Nevertheless, the concentration of INPs in the sea surface microlayer is variable and the efficiency of emitting marine INP from the surface is wind speed dependent (DeMott et al., 2016; Irish et al., 2017; McCluskey et al., 2018; Wilson et al., 2015). Therefore, even though the trajectories on the 27th and 30th interacted with the marine boundary layer, they may contain different concentrations of INPs, yielding the observed differences in n_{mw}. In addition to air mass origin, it has been shown that precipitation efficiently removes INP and thus influences n_{mw} (Stopelli et al., 2015). Indeed, the most upstream precipitation (see Fig. A8) corresponds to the sample collected on the 30th, which has the lowest n_{mw}. Therefore, the most efficient INPs could have been removed in the upstream precipitation, contributing to the observed decrease in n_{mw}.

The differences in n_{mw} could not be rectified by a single metric in this study but rather a combination of factors likely led to the observed variability. In particular, as the warm sector of the cyclone approached the sampling site (28th), n_{mw} increased. Conversely, after cold frontal passage (30th) the n_{mw} decreased. Back trajectories indicate that the air mass source region and the amount of upstream precipitation differed between the two sectors of the cyclone. This result is consistent with previous studies that suggest that air mass origin (e.g. Ault et al., 2011; Creamean et al., 2013; Field et al., 2006; Lacher et al., 2017, 2018) and upstream precipitation (Stopelli et al., 2015) influences the INP concentration. Furthermore, the dependence on the long range air mass history to the observed variability in n_{mw} suggests that local sources are not responsible for the observed INPs.

4.4 Limitations of snow meltwater sample comparisons

One limitation when comparing snow samples collected at different times and locations is the unknown number of aerosols, INPs and ice crystals that contributed to the collected meltwater. Since n_{mw} depends on the number and mass of the ice crystals within a snow sample, the melt water volume or density of each snowflake influences n_{mw}. For example, snow to liquid ratios, which can be used as a proxy for snow flake density and melt water equivalent, can vary between 5 to 1 in heavy wet snow and 100 to 1 in powdery snow (Roebber et al., 2003). However, even when considering this variability in the required amount of snow to produce the same volume of ice crystal melt water, n_{mw} would only differ by a factor of 20. As can be seen in Fig. 10, n_{mw} varies by two orders of magnitude or more between the 28th and the 30th of November and the difference is therefore robust. Additionally, heavy wet snow has been found to occur in the warm core of a synoptic system while lighter, more powdery snow was found in the air mass after cold frontal passage, where air temperatures are colder (Roebber et al., 2003). As the n_{mw} on the 28th was collected in the warm sector and the sample on the 30th was post cold front, differences in snow density may lead to an underestimation in the difference between the n_{mw} of these two samples. Therefore, we recommend that future studies also consider the snow water equivalent when comparing the n_{mw} as this could influence n_{mw} by a factor of 20 or more.

Another uncertainty with using precipitation samples for analyzing INP concentrations is associated with aerosol scavenging and chemical ageing (e.g. ~~(~~Petters and Wright, 2015). As previously mentioned, the samples were stored frozen to avoid any decrease in ice nucleating ability associated with storage (Stopelli et al., 2014) and therefore degradation is likely not an issue in this study (Wex et al., 2019). The ability of a falling ice crystal to scavenge aerosols or rime cloud droplets depends on the ice crystal habit, size, and the difference between the fall velocity of the crystal and the interstitial aerosol or cloud droplets. With the exception of interstitial aerosol concentration which has been shown to influence n_{mw} by a factor of 2 (Petters and Wright, 2015), these factors are all important when estimating snow density and thus make it difficult to disentangle their effects on n_{mw}. Therefore, there is value in future studies of INP in MPCs to investigate the INP concentrations in cloud water, interstitial aerosols and snow samples.

4.5 Ice Nucleating Particle Concentrations in Diluted Snow Samples

In order to extend the reported temperature range of DRINCZ, the snow samples were also diluted by a factor of 10 with SA water (see Eq. 2). The dilutions (open symbols) overlay the pure samples except at the warmest temperatures where, as previously mentioned, a single freezing event can lead to an increase in n_{mw} of an order of magnitude relative to the undiluted sample. This effect is especially evident on the 27th when the first few wells of the diluted sample (open blue circles) froze at the same or higher temperatures than the undiluted sample (filled blue circles) and led to an increase in n_{mw} of up to an order of magnitude. However, this issue has been previously observed when diluting from stock ~~solutions~~ suspensions (Harrison et al., 2018) which is similar to diluting a snow water sample. Therefore, the dilutions further validate DRINCZ as an INP measurement technique.

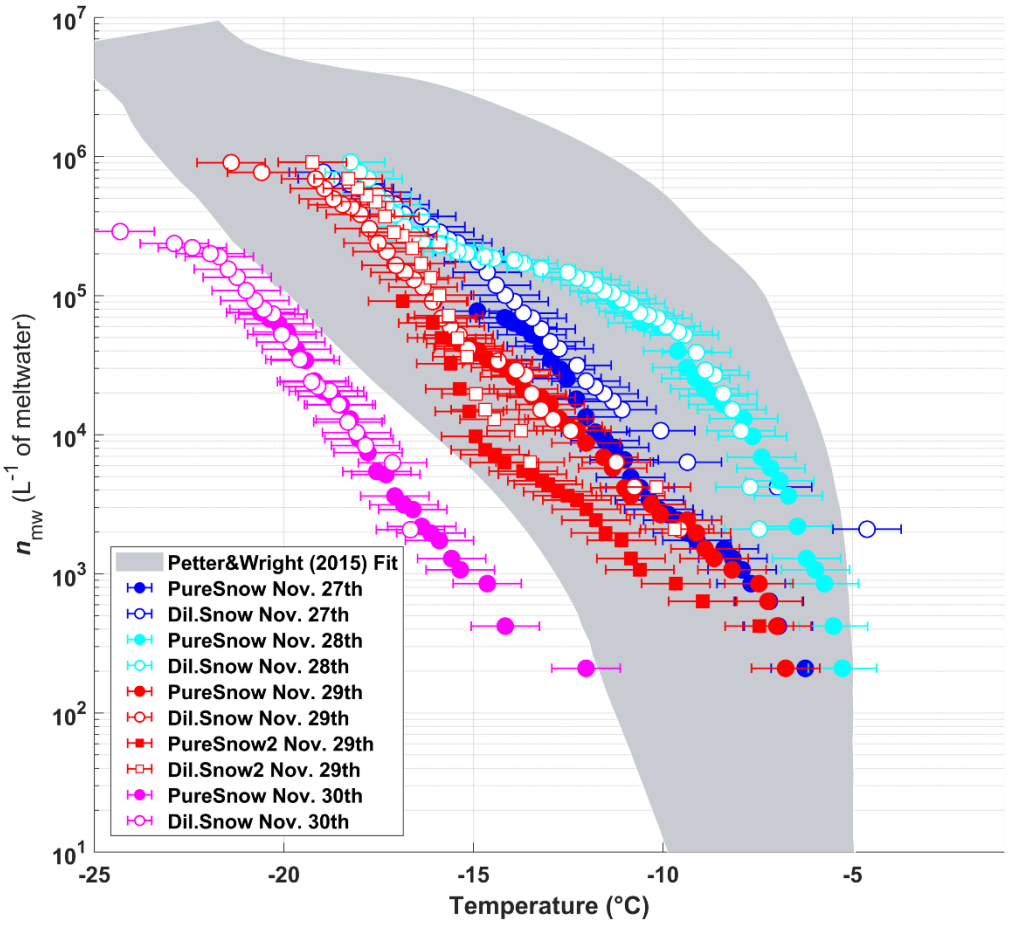

Figure 10: The cumulative number of active sites per L of meltwater (n_{mw}) of snow for undiluted snow (filled) and of snow samples diluted by a factor of 10 (white-filled symbols) as a function of temperature. The colors represent the different sampling days. On the 29th of Nov. two samples were taken and the second sample of the day is indicated by square symbols. The shaded area represents the previously reported n_{mw} from precipitation events as described in Petters and Wright (2015). The error bars represent the instrumental temperature uncertainty of ± 0.9 ˚C.

5 Conclusions

We describe and characterize DRINCZ as a newly developed drop freezing instrument for quantifying the ability of aerosols to act as ice nucleating particles in the immersion freezing mode. The instrument uncertainty is ± 0.9 ˚C, similar to previously published drop freezing techniques. We show that thermal contraction of ethanol as a coolant used in bath-based drop freezing techniques increases temperature variations within the sample. This issue can be corrected by incorporating a bath leveler which ensures the coolant level in the bath remains constant during an experiment. Typical drop freezing methods report temperature measured in the corner wells of a 96-well tray, at the edge of a cooling block or within the block itself (Beall et al., 2017; Hill et al., 2014; Stopelli et al., 2014). Here we show that by making use of the freezing sequence of pure water aliquots, the spatial pattern of temperature bias in the 96-well tray can be assessed. Although variations are within the

instrumental uncertainty of DRINCZ and are not used for DRINCZ data analysis, we present our detailed analysis of this potential bias and draw attention to this issue for other drop freezing techniques. The calculated bias correction increases the precision of drop freezing setups, and is an alternative to computationally expensive heat transfer simulations (Beall et al., 2017). Validation experiments conducted with NX-illite showed good agreement with data reported in the literature for this INP standard.

We exemplify the use of DRINCZ by measuring the concentration of INP in snow samples collected at the Sonnblick Observatory in Austria. The observed INP concentrations are within previously reported values as summarized in Petters and Wright, (2015) for the same temperature range as investigated here (-22 to 0 ˚C). Differences in INP concentration can be explained by differing sectors of a mid-latitude cyclone. As the warm sector of the cyclone approached the sampling site, the INP concentration increased while after the cold front passed the INP concentration decreased. Back trajectories indicate that the air mass source region and the amount of upstream precipitation differed between the two sectors of the cyclone. This result is consistent with previous studies that suggest that air mass origin (e.g. (Ault et al., 2011; Creamean et al., 2013; Field et al., 2006; Lacher et al., 2017) and upstream precipitation (Stopelli et al., 2015) influence the INP concentration. This suggests that INP in precipitation samples are likely transported from specific source regions rather than originate from local sources. Thus identifying the specific sources responsible for INP and their transport pathways are essential for accurately modelling the ice phase in clouds and ultimately, climate.

Author Contributions

DRINCZ was developed and designed by R.O.D with the assistance of M.C.C, M.R., L.S.B, K.P.B and N.B.D. The SA water experiments were conducted by M.C.C, K.P.B., L.S.B, V.W, J.W, S.B, and R.O.D. The temperature calibration and NX-illite experiments were conducted and analyzed by K.P.B and N.B.D. The snow samples were collected by N.E. and analyzed by R.O.D. The instrumental error, uncertainties and calibration were conducted by R.O.D. with contributions from Z.A.K and C.M. The automation and analysis software was developed by R.O.D. with contributions from K.P.B and M.C.C. The well plate holder was designed by M.R. and R.O.D. and manufactured by M.R. The manuscript was written by R.O.D with contributions from N.B.D, C.M. and Z.A.K. The project was supervised by Z.A.K.

Acknowledgements

R.O.D. and Z.A.K. would like to acknowledge funding from SNF grant #200021_156581. Z. A. K. would like to acknowledge Franz Conen and Emillano Stopelli for assistance with the initial set up of the droplet freezing assay. We are grateful to Dr.

James D. Atkinson for discussions and help with experiments during the preparatory phase of DRINCZ development. We acknowledge technical assistance from Hannes Wylder. R.O.D. would like to thank Dr. William Ball for insightful statistical discussions, Ellen Gute for performing camera tests and Michele Gregorini for assistance with the automation.

Appendix A

Freezing bias by user

The 20 SA water experiments were performed over a three month period by two users. The SA water was unaffected by aging over this period as it originated from varying bottles distributed by the manufacturer (Sigma Aldrich). The user bias was calculated the same way as the bias for all 20 experiments. The bias is relative to the median freezing temperature of the 4 corner wells obtained by the respective user. As can be seen in Fig. A3~~2~~, the pattern of freezing bias is consistent regardless of the user. This similarity indicates that the reported bias is instrumental and not user specific.

Bias significance and correction

To ensure that the observed bias is statistically significant, a two-sample, two-tailed *t*-test was performed. In particular, a Welch's *t*-test was used due to the different number of samples between the combination of the 4 reference wells (20 experiments x 4 wells = 80 values) and each well (20 experiments x 1 well = 20 values) and the different variance of freezing for each well (Derrick and White, 2016). In a Welch's *t*-test the location parameter of two independent data samples is assessed as follows:

$$t = \frac{\bar{w}_{4ref} - \bar{w}_i}{\sqrt{\frac{s^2_{4ref}}{Nw_{4ref}} + \frac{s^2_i}{Nw_i}}} \quad \text{(A1)}$$

where $\bar{w}_{4ref}$ and $\bar{w}_i$ are the mean freezing temperature of the reference wells and an individual well, respectively. s^2_{4ref} and s^2_i are the variances of freezing in the reference and the individual wells and Nw_{4ref} and Nw_i are the number of samples for the reference wells and an individual well, respectively. The variance of the freezing temperature of SA water in each well is shown as boxplots in the Appendix (Fig. A2~~3~~). The temperature of approximately 30% of the wells was found to be statistically different from the average freezing temperature of the 4 reference wells at the 95% confidence level, with a resultant mean bias of 0.23 ˚C (Fig. 4b). Due to a fraction of wells with a statistically significant bias, a correction factor based on the mean bias from the 20 SA water experiments is tested for all wells excluding the 4 corner wells used as the reference to avoid overfitting the data. Of note, the reported bias is derived based on the freezing range of SA water from -16 to -26 °C. However, based on the relatively constant spread in the temperature calibration data (see Fig. 3b), it is reasonable to assume that the bias has a weak temperature dependence.

Although the freezing bias was shown to be representative when the SA water data was split in two (8 and 12 samples), it is still necessary to validate its robustness on a larger sample size. In order to artificially increase the sample size of the experiments, the bias was recalculated randomly such that only 90% or 18 of the experiments were used. The resultant bias correction was then applied to the remaining 10% or 2 of the experiments and tested to see if the mean freezing temperature of the bias corrected tray was closer to the reference freezing temperature of the 4 corner wells. This procedure was repeated 1000 times at random. The difference in the median freezing temperature (*FF*= ~~50 %~~0.5) and 4 corner reference wells decreased from 0.23 ˚C to 0.04 ˚C, while the standard deviation of the bias corrected data increased by 0.007 ˚C. Thus, the bias correction performed as expected and reduced the bias in freezing temperature. Nonetheless, this improvement falls within the uncertainty of the instrument, as discussed in Section 3.3 and is therefore not applied to DRINCZ measurements by default.

Synoptic Summary Nov. 27th-30th

The synoptic pattern over Europe on the 27th through 30th of November produced large variations in both temperature and air mass origin at the SBO. As can be seen from the surface pressure maps shown in Fig. A5, an evolving cyclone tracked across Northern Europe before occluding in the vicinity of Denmark. This cyclone produced strong warm advection at SBO on the 27th (see Fig. A7) in advance of the approaching cold front. As the cyclone began to fill over Southern Scandinavia, the cold front stalled along the Alps and westerly flow continued at SBO from the 28th – 29th (Fig. A7). Farther west, the cold front reached the Mediterranean where a secondary low developed along the remnant baroclinic zone (Fig. A6 panel c.). This secondary low traversed Italy and rapidly intensified as it crossed the Adriatic Sea before entering the northern Balkans (Fig. A6 panel d.). The secondary low and an amplifying ridge over the British Isles forced the cold front over SBO at 00Z on the 30th when cold air advection ensued over the SBO region (Fig. A7), as shown by the back trajectories (Fig. A8.e and f.).

HYSPLIT back trajectories

The Hybrid Single-Particle Lagrangian Integrated Trajectory model (HYSPLIT) (Stein et al., 2015) was run using the interactive web portal (Rolph et al., 2017). The trajectories were calculated using 0.5˚ resolution and the trajectories were initialized 1000, 2000 and 3000 meters above the model terrain height. Although the majority of snow mass growth has been shown to occur between mountaintop and 1 km above the surface (Lowenthal et al., 2016), these heights were chosen due to the coarse resolution of the model terrain height and the observed sensitivity of the back trajectories with height. HYSPLIT was initialized using the 0.5˚ hourly Global Data Assimilation System (GDAS) archived database and the vertical velocity was model based rather than isentropic.

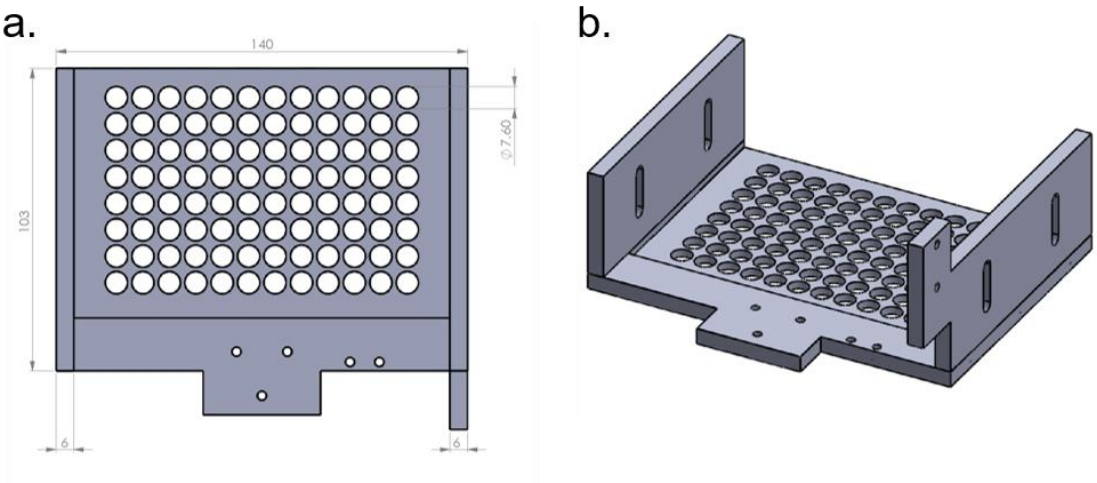

Figure A1: Schematic of the 96-well tray holder from above (a) and the side (b), dimensions are in millimeters.

Figure A2~~3~~. A side by side comparison of box plots for the freezing temperatures of the 20 SA water experiments of the reference wells (left box) and the well represented by the location (right box) of each subplot. The median (red line), inter-quartile range (blue box), extreme values not considered outliers (whiskers) and outliers (red crosses) are shown as a function of temperature in ˚C (y-axes).

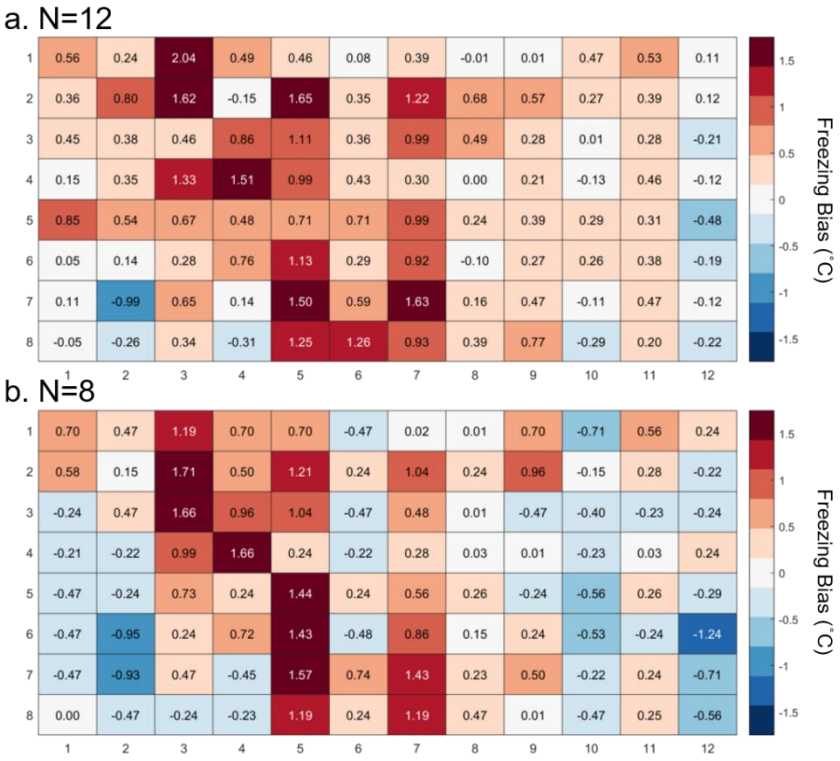

Figure A32: (a) Bias in the freezing of SA water (˚C) based on the median value of each well over 12 experiments and (b) 8 experiments relative to the median temperature of freezing for the 4 corner wells used during the temperature calibration. A positive (negative) bias indicates that the wells experience a warmer (colder) temperature than the four corner wells used for temperature calibration and therefore freeze at lower (higher) temperatures than reported.

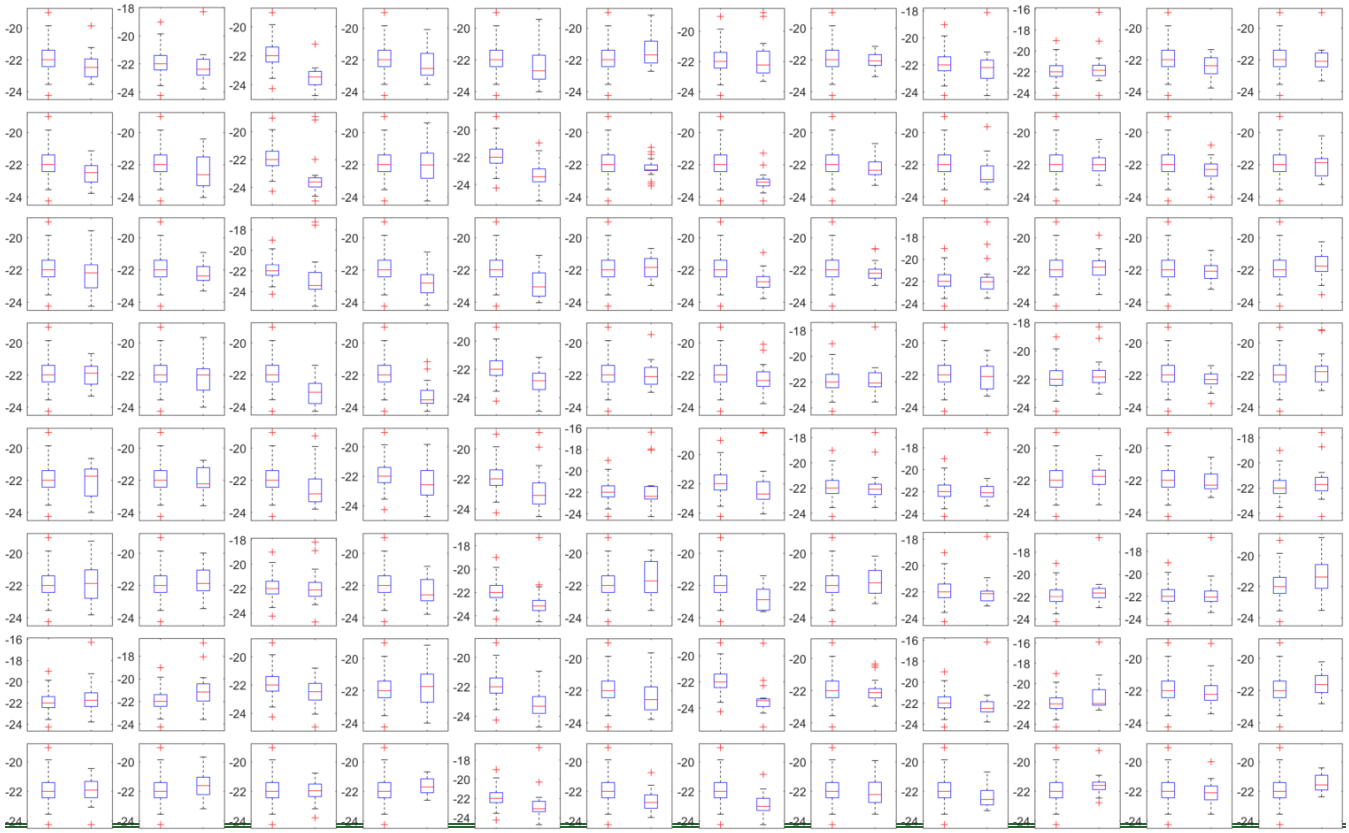

~~**Figure A3. A side by side comparison of box plots for the freezing temperatures of the 20 SA water experiments of the reference wells (left box) and the well represented by the location (right box) of each subplot. The median (red line), inter-quartile range (blue box), extreme values not considered outliers (whiskers) and outliers (red crosses) are shown as a function of temperature in °C (y-axes).**~~

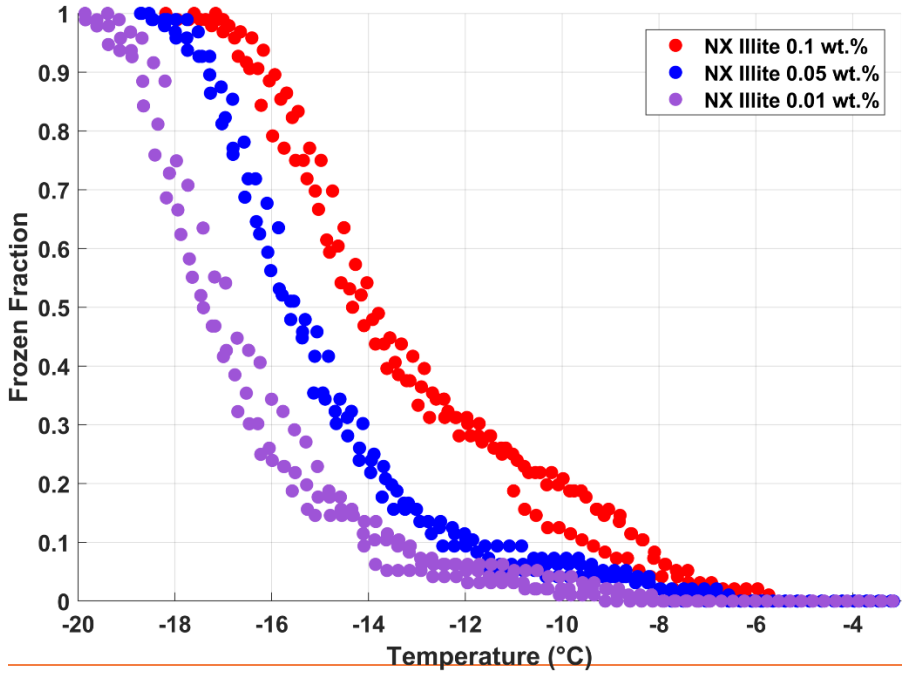

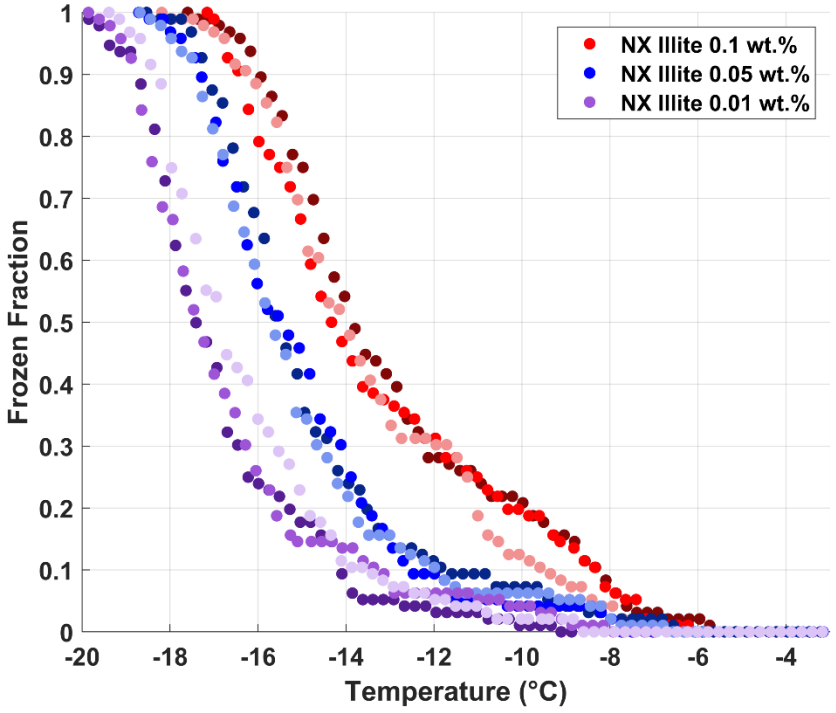

Figure A4. Frozen fraction curves of ~~s~~suspensions~~olutions~~ of 0.01 wt. % (magenta dots), 0.05 wt. % (red dots) and 0.01 wt. % (purple dots) of NX-illite run in triplicates as shown by shading.

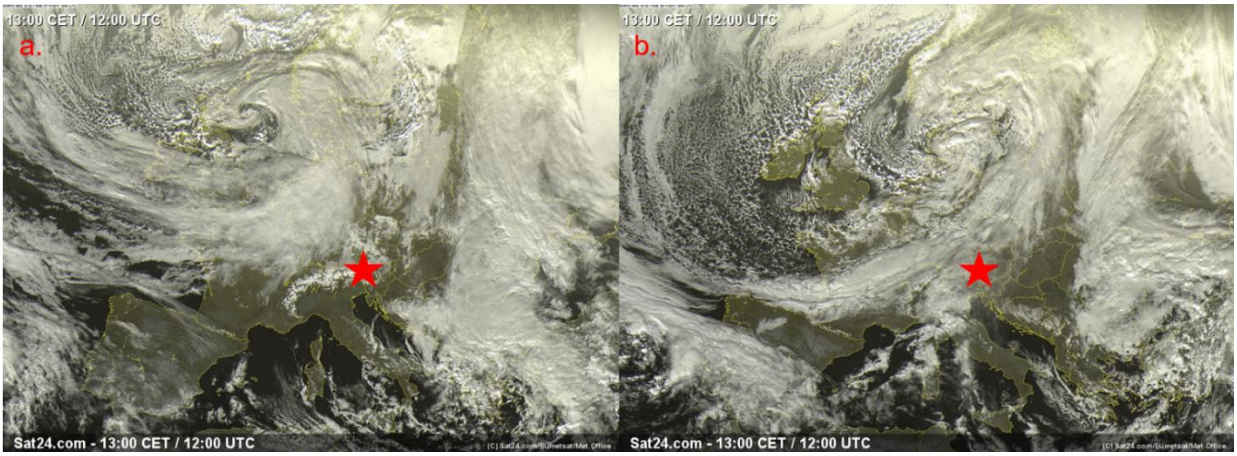

Figure A5: Visible satellite image of the storm system impacting the SBO (red star) taken at 1200UTC on (a) Nov. 27th and (b) 28th. Images courtesy of Sat24.com/Eumetsat/Met Office (http://www.sat24.com/history.aspx).

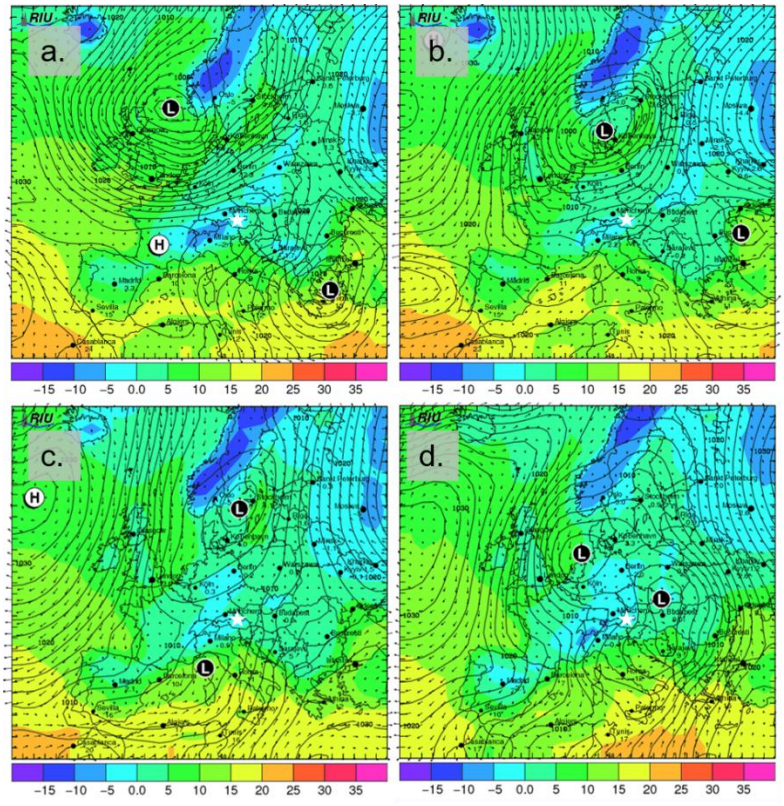

Figure A6: Forecasted surface pressure in hPa (black contours), 2 meter surface temperature in ˚C (color fill), and wind vectors in m/s (black arrows) for 12 UTC on (a) 27th , (b) 28th , (c) 29th and (d) 30th. Forecasts are based on model runs initialized on 00 UTC of the day of interest (12 hours before shown values). Surface low and high pressure centers are indicated with L and H, respectively. The location of SBO is shown by the white star. Images are taken and adapted from the Rhenish Institute for Environmental Research at the University of Cologne (http://www.uni-koeln.de/math-nat-fak/geomet/eurad/index_e.html).

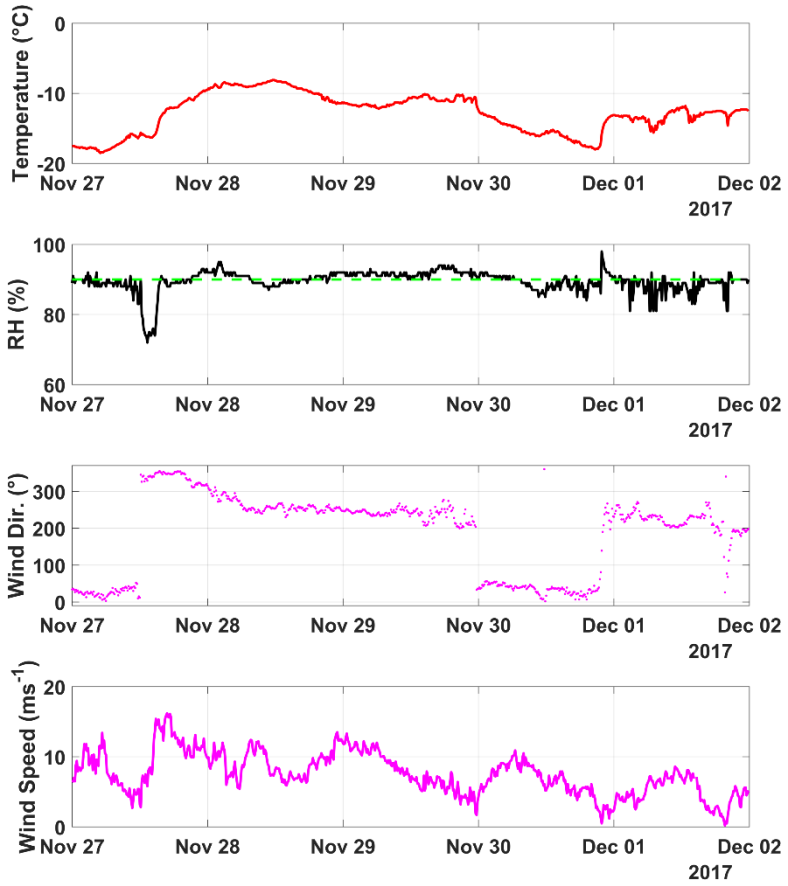

Figure A7: (top panel) Temperature (˚C), (top-middle panel) humidity (%), (bottom-middle panel) wind direction (˚) and (bottom panel) wind speed (ms^{-1}) as a function of date spanning from the 27th of November to the 2nd of December (in UTC). The humidity when cloud is present at SBO (90%) is shown (dashed green line).

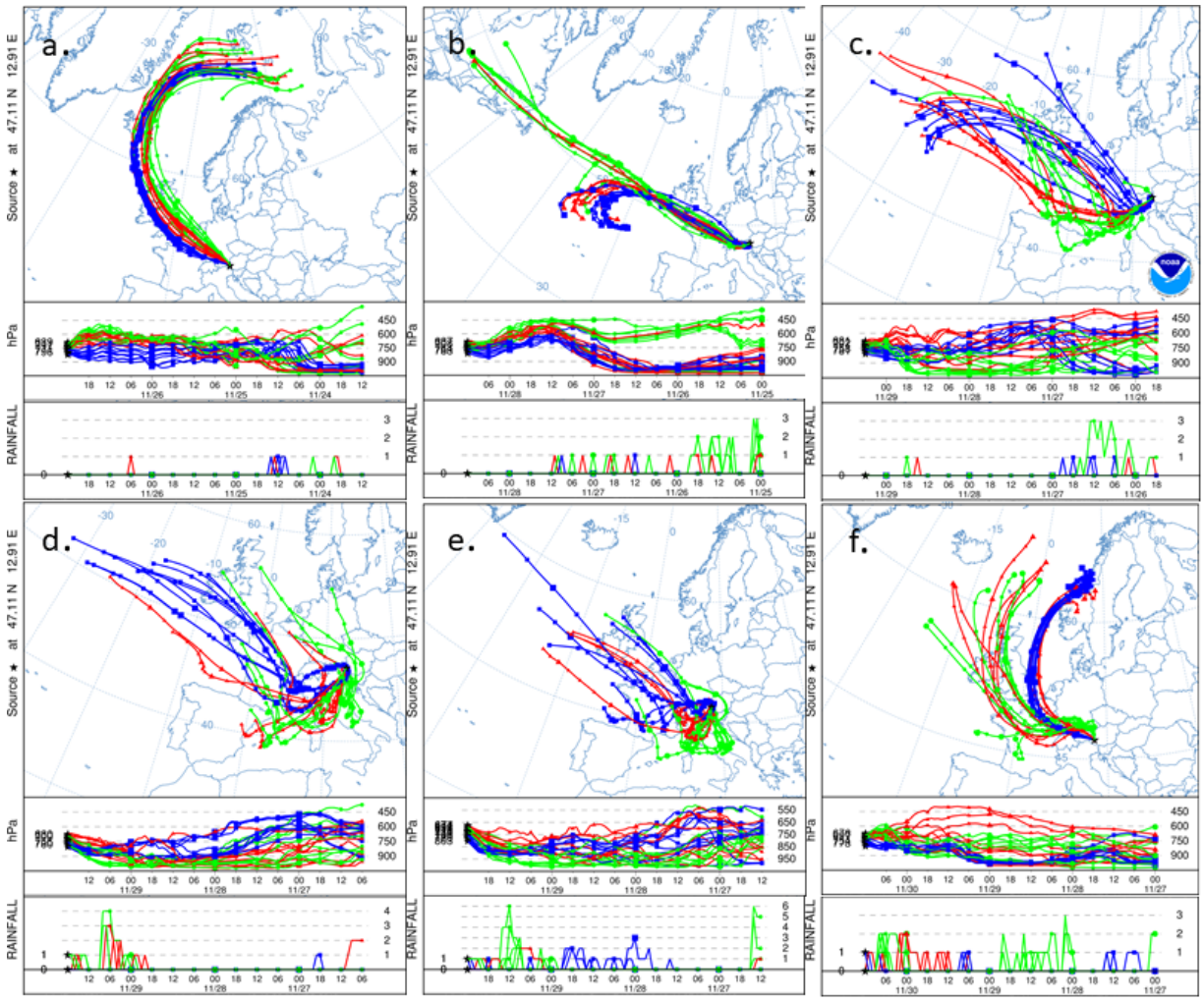

Figure A8: (a) 84-hour HYSPLIT back trajectories from the Sonnblick Observatory initialized on 00 UTC on the 27th, (b) 12 UTC on the 28th, (c) 06 UTC and (d) 18 UTC on the 29th, and (e) 00 UTC and (f) 12 UTC on the 30th of November. The blue, green and red lines represent 8 ensemble back trajectories initialized 1000 m, 2000 m and 3000 m above the model terrain height, respectively. The two lower panels in each subplot show the back trajectory height in units of pressure (hPa) and rainfall (mm) as a function of time (in 6 hourly intervals) as a function of pressure (in hPa).

References

Ansmann, A., Tesche, M., Seifert, P., Althausen, D., Engelmann, R., Fruntke, J., Wandinger, U., Mattis, I. and Müller, D.: Evolution of the ice phase in tropical altocumulus: SAMUM lidar observations over Cape Verde, J. Geophys. Res. Atmospheres, 114(D17), doi:10.1029/2008JD011659, 2009.

Atherton, T. J. and Kerbyson, D. J.: Size Invariant Circle Detection., 1999.

Atkinson, J. D., Murray, B. J., Woodhouse, M. T., Whale, T. F., Baustian, K. J., Carslaw, K. S., Dobbie, S., O'Sullivan, D. and Malkin, T. L.: The importance of feldspar for ice nucleation by mineral dust in mixed-phase clouds, Nature, 498(7454), 355, doi:10.1038/nature12278, 2013.

Ault, A. P., Williams, C. R., White, A. B., Neiman, P. J., Creamean, J. M., Gaston, C. J., Ralph, F. M. and Prather, K. A.: Detection of Asian dust in California orographic precipitation, J. Geophys. Res. Atmospheres, 116(D16), doi:10.1029/2010JD015351, 2011.

Beall, C. M., Stokes, M. D., Hill, T. C., DeMott, P. J., DeWald, J. T. and Prather, K. A.: Automation and heat transfer characterization of immersion mode spectroscopy for analysis of ice nucleating particles, Atmos Meas Tech, 10(7), 2613–2626, doi:10.5194/amt-10-2613-2017, 2017.

Beck, A., Henneberger, J., Fugal, J. P., David, R. O., Lacher, L. and Lohmann, U.: Impact of surface and near-surface processes on ice crystal concentrations measured at mountain-top research stations, Atmospheric Chem. Phys., 18(12), 8909–8927, doi:https://doi.org/10.5194/acp-18-8909-2018, 2018.

Boer, G. de, Morrison, H., Shupe, M. D. and Hildner, R.: Evidence of liquid dependent ice nucleation in high-latitude stratiform clouds from surface remote sensors, Geophys. Res. Lett., 38(1), doi:10.1029/2010GL046016, 2011.

Boose, Y., Welti, A., Atkinson, J., Ramelli, F., Danielczok, A., Bingemer, H. G., Plötze, M., Sierau, B., Kanji, Z. A. and Lohmann, U.: Heterogeneous ice nucleation on dust particles sourced from nine deserts worldwide – Part 1: Immersion freezing, Atmospheric Chem. Phys., 16(23), 15075–15095, doi:https://doi.org/10.5194/acp-16-15075-2016, 2016a.

Boose, Y., Kanji, Z. A., Kohn, M., Sierau, B., Zipori, A., Crawford, I., Lloyd, G., Bukowiecki, N., Herrmann, E., Kupiszewski, P., Steinbacher, M. and Lohmann, U.: Ice Nucleating Particle Measurements at 241 K during Winter Months at 3580 m MSL in the Swiss Alps, J. Atmospheric Sci., 73(5), 2203–2228, doi:10.1175/JAS-D-15-0236.1, 2016b.

Broadley, S. L., Murray, B. J., Herbert, R. J., Atkinson, J. D., Dobbie, S., Malkin, T. L., Condliffe, E. and Neve, L.: Immersion mode heterogeneous ice nucleation by an illite rich powder representative of atmospheric mineral dust, Atmos Chem Phys, 12(1), 287–307, doi:10.5194/acp-12-287-2012, 2012.

Burkert-Kohn, M., Wex, H., Welti, A., Hartmann, S., Grawe, S., Hellner, L., Herenz, P., Atkinson, J. D., Stratmann, F. and Kanji, Z. A.: Leipzig Ice Nucleation chamber Comparison (LINC): intercomparison of four online ice nucleation counters, Atmos Chem Phys, 17(18), 11683–11705, doi:10.5194/acp-17-11683-2017, 2017.

Christner, B. C., Cai, R., Morris, C. E., McCarter, K. S., Foreman, C. M., Skidmore, M. L., Montross, S. N. and Sands, D. C.: Geographic, seasonal, and precipitation chemistry influence on the abundance and activity of biological ice nucleators in rain and snow, Proc. Natl. Acad. Sci., 105(48), 18854–18859, doi:10.1073/pnas.0809816105, 2008.

Creamean, J. M., Suski, K. J., Rosenfeld, D., Cazorla, A., DeMott, P. J., Sullivan, R. C., White, A. B., Ralph, F. M., Minnis, P., Comstock, J. M., Tomlinson, J. M. and Prather, K. A.: Dust and Biological Aerosols from the Sahara and Asia Influence Precipitation in the Western U.S., Science, 339(6127), 1572–1578, doi:10.1126/science.1227279, 2013.

Cziczo, D. J., Ladino, L., Boose, Y., Kanji, Z. A., Kupiszewski, P., Lance, S., Mertes, S. and Wex, H.: Measurements of Ice Nucleating Particles and Ice Residuals, Meteorol. Monogr., 58, 8.1-8.13, doi:10.1175/AMSMONOGRAPHS-D-16-0008.1, 2017.

DeMott, P. J., Cziczo, D. J., Prenni, A. J., Murphy, D. M., Kreidenweis, S. M., Thomson, D. S., Borys, R. and Rogers, D. C.: Measurements of the concentration and composition of nuclei for cirrus formation, Proc. Natl. Acad. Sci. U. S. A., 100(25), 14655–14660, doi:10.1073/pnas.2532677100, 2003.

DeMott, P. J., Prenni, A. J., McMeeking, G. R., Sullivan, R. C., Petters, M. D., Tobo, Y., Niemand, M., Möhler, O., Snider, J. R., Wang, Z. and Kreidenweis, S. M.: Integrating laboratory and field data to quantify the immersion freezing ice nucleation activity of mineral dust particles, Atmospheric Chem. Phys., 15(1), 393–409, doi:10.5194/acp-15-393-2015, 2015.

DeMott, P. J., Hill, T. C. J., McCluskey, C. S., Prather, K. A., Collins, D. B., Sullivan, R. C., Ruppel, M. J., Mason, R. H., Irish, V. E., Lee, T., Hwang, C. Y., Rhee, T. S., Snider, J. R., McMeeking, G. R., Dhaniyala, S., Lewis, E. R., Wentzell, J. J. B., Abbatt, J., Lee, C., Sultana, C. M., Ault, A. P., Axson, J. L., Martinez, M. D., Venero, I., Santos-Figueroa, G., Stokes, M. D., Deane, G. B., Mayol-Bracero, O. L., Grassian, V. H., Bertram, T. H., Bertram, A. K., Moffett, B. F. and Franc, G. D.: Sea spray aerosol as a unique source of ice nucleating particles, Proc. Natl. Acad. Sci., 113(21), 5797–5803, doi:10.1073/pnas.1514034112, 2016.

DeMott, P. J., Hill, T. C. J., Petters, M. D., Bertram, A. K., Tobo, Y., Mason, R. H., Suski, K. J., McCluskey, C. S., Levin, E. J. T., Schill, G. P., Boose, Y., Rauker, A. M., Miller, A. J., Zaragoza, J., Rocci, K., Rothfuss, N. E., Taylor, H. P., Hader, J. D., Chou, C., Huffman, J. A., Pöschl, U., Prenni, A. J. and Kreidenweis, S. M.: Comparative measurements of ambient atmospheric concentrations of ice nucleating particles using multiple immersion freezing methods and a continuous flow diffusion chamber, Atmospheric Chem. Phys., 17(18), 11227–11245, doi:10.5194/acp-17-11227-2017, 2017.

Derrick, B. and White, P.: Why Welch' s test is Type I error robust, Quant. Methods Psychol., 12, 30–38, doi:10.20982/tqmp.12.1.p030, 2016.

Felgitsch, L., Baloh, P., Burkart, J., Mayr, M., Momken, M. E., Seifried, T. M., Winkler, P., Schmale III, D. G. and Grothe, H.: Birch leaves and branches as a source of ice-nucleating macromolecules, Atmospheric Chem. Phys., 18(21), 16063–16079, doi:https://doi.org/10.5194/acp-18-16063-2018, 2018.

Field, P. R., Möhler, O., Connolly, P., Krämer, M., Cotton, R., Heymsfield, A. J., Saathoff, H. and Schnaiter, M.: Some ice nucleation characteristics of Asian and Saharan desert dust, Atmos Chem Phys, 6(10), 2991–3006, doi:10.5194/acp-6-2991-2006, 2006.

Fletcher, N. H.: The physics of rainclouds, Cambridge University Press., 1962.

Harrison, A. D., Whale, T. F., Rutledge, R., Lamb, S., Tarn, M. D., Porter, G. C. E., Adams, M. P., McQuaid, J. B., Morris, G. J. and Murray, B. J.: An instrument for quantifying heterogeneous ice nucleation in multiwell plates using infrared emissions to detect freezing, Atmospheric Meas. Tech., 11(10), 5629–5641, doi:https://doi.org/10.5194/amt-11-5629-2018, 2018.

Hartmann, S., Niedermeier, D., Voigtländer, J., Clauss, T., Shaw, R. A., Wex, H., Kiselev, A. and Stratmann, F.: Homogeneous and heterogeneous ice nucleation at LACIS: operating principle and theoretical studies, Atmos Chem Phys, 11(4), 1753–1767, doi:10.5194/acp-11-1753-2011, 2011.

Hill, T. C. J., Moffett, B. F., DeMott, P. J., Georgakopoulos, D. G., Stump, W. L. and Franc, G. D.: Measurement of Ice Nucleation-Active Bacteria on Plants and in Precipitation by Quantitative PCR, Appl. Environ. Microbiol., 80(4), 1256–1267, doi:10.1128/AEM.02967-13, 2014.

Hiranuma, N., Augustin-Bauditz, S., Bingemer, H., Budke, C., Curtius, J., Danielczok, A., Diehl, K., Dreischmeier, K., Ebert, M., Frank, F., Hoffmann, N., Kandler, K., Kiselev, A., Koop, T., Leisner, T., Möhler, O., Nillius, B., Peckhaus, A., Rose, D., Weinbruch, S., Wex, H., Boose, Y., DeMott, P. J., Hader, J. D., Hill, T. C. J., Kanji, Z. A., Kulkarni, G., Levin, E. J. T., McCluskey, C. S., Murakami, M., Murray, B. J., Niedermeier, D., Petters, M. D., O'Sullivan, D., Saito, A., Schill, G. P., Tajiri, T., Tolbert, M. A., Welti, A., Whale, T. F., Wright, T. P. and Yamashita, K.: A comprehensive laboratory study on the immersion freezing behavior of illite NX particles: a comparison of 17 ice nucleation measurement techniques, Atmos Chem Phys, 15(5), 2489–2518, doi:10.5194/acp-15-2489-2015, 2015.

Hiranuma, N., Adachi, K., Bell, D. M., Belosi, F., Beydoun, H., Bhaduri, B., Bingemer, H., Budke, C., Clemen, H.-C., Conen, F., Cory, K. M., Curtius, J., DeMott, P. J., Eppers, O., Grawe, S., Hartmann, S., Hoffmann, N., Höhler, K., Jantsch, E., Kiselev, A., Koop, T., Kulkarni, G., Mayer, A., Murakami, M., Murray, B. J., Nicosia, A., Petters, M. D., Piazza, M., Polen, M., Reicher, N., Rudich, Y., Saito, A., Santachiara, G., Schiebel, T., Schill, G. P., Schneider, J., Segev, L., Stopelli, E., Sullivan, R. C., Suski, K., Szakáll, M., Tajiri, T., Taylor, H., Tobo, Y., Ullrich, R., Weber, D., Wex, H., Whale, T. F., Whiteside, C. L., Yamashita, K., Zelenyuk, A. and Möhler, O.: A comprehensive characterization of ice nucleation by three different types of cellulose particles immersed in water, Atmospheric Chem. Phys., 19(7), 4823–4849, doi:https://doi.org/10.5194/acp-19-4823-2019, 2019.

Hoose, C. and Möhler, O.: Heterogeneous ice nucleation on atmospheric aerosols: a review of results from laboratory experiments, Atmos Chem Phys, 12(20), 9817–9854, doi:10.5194/acp-12-9817-2012, 2012.

Irish, V. E., Elizondo, P., Chen, J., Chou, C., Charette, J., Lizotte, M., Ladino, L. A., Wilson, T. W., Gosselin, M., Murray, B. J., Polishchuk, E., Abbatt, J. P. D., Miller, L. A. and Bertram, A. K.: Ice-nucleating particles in Canadian Arctic sea-surface microlayer and bulk seawater, Atmos Chem Phys, 17(17), 10583–10595, doi:10.5194/acp-17-10583-2017, 2017.

Kanji, Z. A., Ladino, L. A., Wex, H., Boose, Y., Burkert-Kohn, M., Cziczo, D. J. and Krämer, M.: Overview of Ice Nucleating Particles, Meteorol. Monogr., 58, 1.1-1.33, doi:10.1175/AMSMONOGRAPHS-D-16-0006.1, 2017.

Kaufmann, L., Marcolli, C., Hofer, J., Pinti, V., Hoyle, C. R. and Peter, T.: Ice nucleation efficiency of natural dust samples in the immersion mode, Atmospheric Chem. Phys., 16(17), 11177–11206, doi:https://doi.org/10.5194/acp-16-11177-2016, 2016.

Kohn, M., Lohmann, U., Welti, A. and Kanji, Z. A.: Immersion mode ice nucleation measurements with the new Portable Immersion Mode Cooling chAmber (PIMCA), J. Geophys. Res. Atmospheres, 121(9), 4713–4733, doi:10.1002/2016JD024761, 2016.

Lacher, L., Lohmann, U., Boose, Y., Zipori, A., Herrmann, E., Bukowiecki, N., Steinbacher, M. and Kanji, Z. A.: The Horizontal Ice Nucleation Chamber (HINC): INP measurements at conditions relevant for mixed-phase clouds at the High Altitude Research Station Jungfraujoch, Atmospheric Chem. Phys., 17(24), 15199–15224, doi:https://doi.org/10.5194/acp-17-15199-2017, 2017.

Lacher, L., Steinbacher, M., Bukowiecki, N., Herrmann, E., Zipori, A. and Kanji, Z. A.: Impact of Air Mass Conditions and Aerosol Properties on Ice Nucleating Particle Concentrations at the High Altitude Research Station Jungfraujoch, Atmosphere, 9(9), 363, doi:10.3390/atmos9090363, 2018.

Lohmann, U. and Feichter, J.: Global indirect aerosol effects: a review, Atmos Chem Phys, 5(3), 715–737, doi:10.5194/acp-5-715-2005, 2005.

Lowenthal, D., Hallar, A. G., McCubbin, I., David, R., Borys, R., Blossey, P., Muhlbauer, A., Kuang, Z. and Moore, M.: Isotopic Fractionation in Wintertime Orographic Clouds, J. Atmospheric Ocean. Technol., 33(12), 2663–2678, doi:10.1175/JTECH-D-15-0233.1, 2016.

752 Lüönd, F., Stetzer, O., Welti, A. and Lohmann, U.: Experimental study on the ice nucleation ability of size-selected kaolinite
753 particles in the immersion mode, J. Geophys. Res. Atmospheres, 115(D14), doi:10.1029/2009JD012959, 2010.

754 Marcolli, C., Gedamke, S., Peter, T. and Zobrist, B.: Efficiency of immersion mode ice nucleation on surrogates of mineral
755 dust, Atmos Chem Phys, 7(19), 5081–5091, doi:10.5194/acp-7-5081-2007, 2007.

756 Matus, A. V. and L'Ecuyer, T. S.: The role of cloud phase in Earth's radiation budget, J. Geophys. Res. Atmospheres, 122(5),
757 2559–2578, doi:10.1002/2016JD025951, 2017.

758 McCluskey, C. S., Ovadnevaite, J., Rinaldi, M., Atkinson, J., Belosi, F., Ceburnis, D., Marullo, S., Hill, T. C. J., Lohmann, U.,
759 Kanji, Z. A., O'Dowd, C., Kreidenweis, S. M. and DeMott, P. J.: Marine and Terrestrial Organic Ice-Nucleating Particles in
760 Pristine Marine to Continentally Influenced Northeast Atlantic Air Masses, J. Geophys. Res. Atmospheres, 123(11), 6196–
761 6212, doi:10.1029/2017JD028033, 2018.

762 Mülmenstädt, J., Sourdeval, O., Delanoë, J. and Quaas, J.: Frequency of occurrence of rain from liquid-, mixed-, and ice-phase
763 clouds derived from A-Train satellite retrievals: RAIN FROM LIQUID- AND ICE-PHASE CLOUDS, Geophys. Res. Lett.,
764 42(15), 6502–6509, doi:10.1002/2015GL064604, 2015.

765 Murray, B. J., L. Broadley, S., W. Wilson, T., J. Bull, S., H. Wills, R., K. Christenson, H. and J. Murray, E.: Kinetics of the
766 homogeneous freezing of water, Phys. Chem. Chem. Phys., 12(35), 10380–10387, doi:10.1039/C003297B, 2010.

767 Murray, B. J., O'Sullivan, D., D. Atkinson, J. and E. Webb, M.: Ice nucleation by particles immersed in supercooled cloud
768 droplets, Chem. Soc. Rev., 41(19), 6519–6554, doi:10.1039/C2CS35200A, 2012.

769 Niemand, M., Möhler, O., Vogel, B., Vogel, H., Hoose, C., Connolly, P., Klein, H., Bingemer, H., DeMott, P., Skrotzki, J. and
770 Leisner, T.: A Particle-Surface-Area-Based Parameterization of Immersion Freezing on Desert Dust Particles, J. Atmospheric
771 Sci., 69(10), 3077–3092, doi:10.1175/JAS-D-11-0249.1, 2012.

772 Petters, M. D. and Wright, T. P.: Revisiting ice nucleation from precipitation samples, Geophys. Res. Lett., 42(20), 8758–
773 8766, doi:10.1002/2015GL065733, 2015.

774 Pinti, V., Marcolli, C., Zobrist, B., Hoyle, C. R. and Peter, T.: Ice nucleation efficiency of clay minerals in the immersion
775 mode, Atmospheric Chem. Phys., 12(13), 5859–5878, doi:https://doi.org/10.5194/acp-12-5859-2012, 2012.

776 Polen, M., Brubaker, T., Somers, J. and Sullivan, R. C.: Cleaning up our water: reducing interferences from non-homogeneous
777 freezing of <q>pure</q> water in droplet freezing assays of ice nucleating particles, Atmospheric Meas. Tech. Discuss., 1–31,
778 doi:https://doi.org/10.5194/amt-2018-134, 2018.

779 Pummer, B. G., Bauer, H., Bernardi, J., Bleicher, S. and Grothe, H.: Suspendable macromolecules are responsible for ice
780 nucleation activity of birch and conifer pollen, Atmos Chem Phys, 12(5), 2541–2550, doi:10.5194/acp-12-2541-2012, 2012.

781 Puxbaum, H. and Tscherwenka, W.: Relationships of major ions in snow fall and rime at sonnblick observatory (SBO, 3106m)
782 and implications for scavenging processes in mixed clouds, Atmos. Environ., 32(23), 4011–4020, doi:10.1016/S1352-
783 2310(98)00244-1, 1998.

784 Reicher, N., Segev, L. and Rudich, Y.: The WeIzmann Supercooled Droplets Observation on a Microarray (WISDOM) and
785 application for ambient dust, Atmos Meas Tech, 11(1), 233–248, doi:10.5194/amt-11-233-2018, 2018.

786 Richardson, M. S., DeMott, P. J., Kreidenweis, S. M., Cziczo, D. J., Dunlea, E. J., Jimenez, J. L., Thomson, D. S., Ashbaugh,
787 L. L., Borys, R. D., Westphal, D. L., Casuccio, G. S. and Lersch, T. L.: Measurements of heterogeneous ice nuclei in the

western United States in springtime and their relation to aerosol characteristics, J. Geophys. Res. Atmospheres, 112(D2), D02209, doi:10.1029/2006JD007500, 2007.

Riechers, B., Wittbracht, F., H?tten, A. and Koop, T.: The homogeneous ice nucleation rate of water droplets produced in a microfluidic device and the role of temperature uncertainty, Phys. Chem. Chem. Phys., 15(16), 5873, doi:10.1039/c3cp42437e, 2013.

Roebber, P. J., Bruening, S. L., Schultz, D. M. and Cortinas, J. V.: Improving Snowfall Forecasting by Diagnosing Snow Density, Weather Forecast., 18(2), 264–287, doi:10.1175/1520-0434(2003)018<0264:ISFBDS>2.0.CO;2, 2003.

Rogers, D. C.: Development of a continuous flow thermal gradient diffusion chamber for ice nucleation studies, Atmospheric Res., 22(2), 149–181, doi:10.1016/0169-8095(88)90005-1, 1988.

Rolph, G., Stein, A. and Stunder, B.: Real-time Environmental Applications and Display sYstem: READY, Environ. Model. Softw., 95, 210–228, doi:10.1016/j.envsoft.2017.06.025, 2017.

Spiess, A.-N., Feig, C. and Ritz, C.: Highly accurate sigmoidal fitting of real-time PCR data by introducing a parameter for asymmetry, BMC Bioinformatics, 9, 221, doi:10.1186/1471-2105-9-221, 2008.

Stan, C. A., Schneider, G. F., Shevkoplyas, S. S., Hashimoto, M., Ibanescu, M., Wiley, B. J. and Whitesides, G. M.: A microfluidic apparatus for the study of ice nucleation in supercooled water drops, Lab. Chip, 9(16), 2293–2305, doi:10.1039/B906198C, 2009.

Stein, A. F., Draxler, R. R., Rolph, G. D., Stunder, B. J. B., Cohen, M. D. and Ngan, F.: NOAA's HYSPLIT Atmospheric Transport and Dispersion Modeling System, Bull. Am. Meteorol. Soc., 96(12), 2059–2077, doi:10.1175/BAMS-D-14-00110.1, 2015.

Stetzer, O., Baschek, B., Lüönd, F. and Lohmann, U.: The Zurich Ice Nucleation Chamber (ZINC)-A New Instrument to Investigate Atmospheric Ice Formation, Aerosol Sci. Technol., 42(1), 64–74, doi:10.1080/02786820701787944, 2008.

Stopelli, E., Conen, F., Zimmermann, L., Alewell, C. and Morris, C. E.: Freezing nucleation apparatus puts new slant on study of biological ice nucleators in precipitation, Atmospheric Meas. Tech., 7(1), 129–134, doi:10.5194/amt-7-129-2014, 2014.

Stopelli, E., Conen, F., Morris, C. E., Herrmann, E., Bukowiecki, N. and Alewell, C.: Ice nucleation active particles are efficiently removed by precipitating clouds, Sci. Rep., 5, 16433, doi:10.1038/srep16433, 2015.

Tan, I., Storelvmo, T. and Zelinka, M. D.: Observational constraints on mixed-phase clouds imply higher climate sensitivity, Science, 352(6282), 224–227, doi:10.1126/science.aad5300, 2016.

Tarn, M. D., Sikora, S. N. F., Porter, G. C. E., O'Sullivan, D., Adams, M., Whale, T. F., Harrison, A. D., Vergara-Temprado, J., Wilson, T. W., Shim, J. and Murray, B. J.: The study of atmospheric ice-nucleating particles via microfluidically generated droplets, Microfluid. Nanofluidics, 22(5), doi:10.1007/s10404-018-2069-x, 2018.

Vali, G.: Quantitative Evaluation of Experimental Results an the Heterogeneous Freezing Nucleation of Supercooled Liquids, J. Atmospheric Sci., 28(3), 402–409, doi:10.1175/1520-0469(1971)028<0402:QEOERA>2.0.CO;2, 1971.

Vali, G.: Revisiting the differential freezing nucleus spectra derived from drop-freezing experiments: methods of calculation, applications, and confidence limits, Atmospheric Meas. Tech., 12(2), 1219–1231, doi:https://doi.org/10.5194/amt-12-1219-2019, 2019.

Vali, G. and Upper, C. D.: Principles of Ice Nucleation, in Biological Ice Nucleation and Its Applications, edited by R. E. Lee, G. J. Warren, and L. V. Gusta, p. 370, The American Phytopathological Society, St. Paul, Minnesota, USA. [online] Available from: https://www.loot.co.za/product/richard-e-lee-biological-ice-nucleation-and-its-applica/wxrm-421-gaa0 (Accessed 16 September 2019), 1995.

Vali, G., DeMott, P. J., Möhler, O. and Whale, T. F.: Technical Note: A proposal for ice nucleation terminology, Atmospheric Chem. Phys., 15(18), 10263–10270, doi:10.5194/acp-15-10263-2015, 2015.

Welti, A., Müller, K., Fleming, Z. L. and Stratmann, F.: Concentration and variability of ice nuclei in the subtropical maritime boundary layer, Atmos Chem Phys, 18(8), 5307–5320, doi:10.5194/acp-18-5307-2018, 2018.

Westbrook, C. D. and Illingworth, A. J.: Evidence that ice forms primarily in supercooled liquid clouds at temperatures > −27°C, Geophys. Res. Lett., 38(14), doi:10.1029/2011GL048021, 2011.

Wex, H., Augustin-Bauditz, S., Boose, Y., Budke, C., Curtius, J., Diehl, K., Dreyer, A., Frank, F., Hartmann, S., Hiranuma, N., Jantsch, E., Kanji, Z. A., Kiselev, A., Koop, T., Möhler, O., Niedermeier, D., Nillius, B., Rösch, M., Rose, D., Schmidt, C., Steinke, I. and Stratmann, F.: Intercomparing different devices for the investigation of ice nucleating particles using Snomax® as test substance, Atmospheric Chem. Phys., 15(3), 1463–1485, doi:10.5194/acp-15-1463-2015, 2015.

Wex, H., Huang, L., Zhang, W., Hung, H., Traversi, R., Becagli, S., Sheesley, R. J., Moffett, C. E., Barrett, T. E., Bossi, R., Skov, H., Hünerbein, A., Lubitz, J., Löffler, M., Linke, O., Hartmann, M., Herenz, P. and Stratmann, F.: Annual variability of ice-nucleating particle concentrations at different Arctic locations, Atmospheric Chem. Phys., 19(7), 5293–5311, doi:https://doi.org/10.5194/acp-19-5293-2019, 2019.

Whale, T. F., Murray, B. J., O'Sullivan, D., Wilson, T. W., Umo, N. S., Baustian, K. J., Atkinson, J. D., Workneh, D. A. and Morris, G. J.: A technique for quantifying heterogeneous ice nucleation in microlitre supercooled water droplets, Atmospheric Meas. Tech., 8(6), 2437–2447, doi:10.5194/amt-8-2437-2015, 2015.

Wilson, T. W., Ladino, L. A., Alpert, P. A., Breckels, M. N., Brooks, I. M., Browse, J., Burrows, S. M., Carslaw, K. S., Huffman, J. A., Judd, C., Kilthau, W. P., Mason, R. H., McFiggans, G., Miller, L. A., Nájera, J. J., Polishchuk, E., Rae, S., Schiller, C. L., Si, M., Temprado, J. V., Whale, T. F., Wong, J. P. S., Wurl, O., Yakobi-Hancock, J. D., Abbatt, J. P. D., Aller, J. Y., Bertram, A. K., Knopf, D. A. and Murray, B. J.: A marine biogenic source of atmospheric ice-nucleating particles, Nature, 525(7568), 234, doi:10.1038/nature14986, 2015.

Reviewer comments on "**Development of the DRoplet Ice Nuclei Counter Zürich (DRINCZ):Validation and application to field collected snow samples**" by Robert O. David, Maria Cascajo Castresana, Killian P. Brennan, Michael Rösch, Nora Els, Julia Werz, Vera Weichlinger, Lin S. Boynton, Sophie Bogler, Nadine Borduas-Dedekind, Claudia Marcolli, Zamin A. Kanji
By Gabor Vali

General:

This paper is a good addition to the literature on INP measurements. Not fundamentally new, but every implementation of the drop-freezing technique, or of any other method, brings new challenges and new ways of solving them. The authors deal with those challenges reasonably well. This paper stands out with its focus on evaluating instrument-caused uncertainties. There are some parts of that evaluation that would benefit from a second look.

We would like to thank Gabor Vali for his positive and very helpful comments and respond to the individual concerns below. Reviewer comments have been reproduced in bold typeface, and author responses are in regular font. All line numbers in authors' response refer to the revised manuscript.

Detailed comments:

41-57 In describing different approaches to INP detection it is useful to separate those that examine air samples and those that take water samples.

In lines 41-56, we are describing single particle methods, which use aerosolized samples that can either be dry dispersed or atomized from a suspension. We now clarify this in lines 51-52. Thus, they can be used to investigate air samples, suspensions or seawater samples. Furthermore, we add "*immerse the samples in water and*" to line 60 to show that bulk methods use samples suspended in solution.

81 Does Bigg (1953) contain data and hail and snow samples? Please check.

Thank you for pointing this out. Indeed, Bigg, (1953) does not use or describe a bulk method to investigate INPs. The citation has been removed from line 83 (revised manuscript).

88 - 89 The goals are stated in overly broad terms. The proposed measurement are expected to be relevant to MPC clouds but no claim should be made that they examine those responsible for ice formation in those cloud. There are other elements to that story beyond the INP measurements. Also, to what degree can these measurements illuminate 'fundamental understanding' of ice nucleation?

We have reformulated the sentence to more explicitly describe the motivation behind the development of DRINCZ. The sentence now reads (90-94): *"In order to further quantify the variability of ambient INP concentration relevant for ice formation in MPCs and increase the understanding of the ice nucleation ability of laboratory and field collected samples, we developed and characterized the DRoplet Ice Nuclei Counter Zurich (DRINCZ). DRINCZ is a drop freezing instrument to investigate ice nucleation at temperature conditions between -25 ˚C and 0 ˚C, representative for MPCs."*

97 In addition to those cited, a design much like the one in this paper was described by Vali (1995; Principles of ice nucleation. Chapter 1 in: "Biological Ice Nucleation and Its Applications", R. E. Lee Jr, G. J. Warren, and L. V. Gusta, Eds., APS Press, The American Phytopathological Society., St. Paul, Minnesota, USA. 370 pp.; ISBN: 0-89054-172-8).

Thank you, we have now added the citation to the text (line 101).

103 Is the foil seal enough to exclude ethanol vapors from getting into the samples and thereby producing a freezing point depression?

This is a valid concern but we believe is not an issue in our experiments. The comparison with literature values of NX-Illite as shown in Fig. 9 do not show a significant bias when compared to techniques that use a sealed cooling block where exposure to ethanol vapors is not an issue. Furthermore, the foil seals used with DRINCZ are non-permeable, suggesting that the probability of ethanol vapors entering the wells would be negligible. To clarify this, we have added "non-permeable" to the description of the foil (line 107).

123 -> Since the position of the sample tray is fixed, and so is its dimension, why is such an elaborate process necessary for identifying the well locations?

As DRINCZ is meant to be a field deployable instrument, the camera mounting location is variable. Even if it is mounted as reproducibly as possible, there are still some variations that can lead to issues when using a fixed well location. Therefore, the code looks for the wells instead of hard coding their locations. This justification is provided at the start of section 2.1.1, lines 129-132 (124-127 in original manuscript).

> **Also, if done this way, to what extent does perspective from the camera lens distorts the circular shape of the wells near the edges of the tray?**
>
> This is a valid point and some edge effects can be seen in Fig. 2a. Nevertheless, the change in light transmission through the well is still significant enough to be detected by the camera to overcome the distortion and shading from edge effects and therefore provide an accurate freezing temperature.

131-132 The meaning of " .... centered at the edge ... as the well center." could probably be clarified better.

Thank you for pointing out that this is confusing. We have therefore reworded the sentences and the preceding sentence to state:" *The CHT first identifies pixels along regions of large gradients in*

brightness to identify pixels at the edge of the well. To determine the center of each well, the algorithm draws circles of varying diameter (ranging between 15 and 30 pixels in diameter, which corresponds to the observed diameters of a well in terms of pixel number) around these edge pixels and classifies the pixel intersecting the largest number of circles as the well center." (lines 135-138)

135 Random order and sorting seem unnecessary with the fixed geometrical arrangement of this setup. What is the rationale here?

As described on lines 129-132 (lines 123-125 in original manuscript), the location of the camera is not fixed in the current setup and can be removed for easier packing and shipping. Therefore, the well locations are not hard coded into the software but rather identified using the CHT. However, future versions of DRINCZ could attempt to have a perfectly reproducible camera location and mounting system so that this would not be needed anymore.

152 Isn't the first instant of intensity change over a threshold magnitude sufficient to detect nucleation? If not so, why not? What possible reason exists for a significant peak in the signal, comparable to that caused by nucleation, prior to nucleation?

The threshold proved to be necessary to account for fluctuations in the light transmission through a well due to turbulence and air entering the ethanol bath. The noise arising due to these fluctuations can be seen in panels b and c of Fig. 2.

157 What is meant by "all recorded images"?

We simply mean all images, and have removed "recorded" from the revised manuscript so as to simply mean all of the images of a well (see line 165)

Fig 2. It is unclear to me what mean intensity and normalized intensity refer to. Is it an average within the circle for a given well? Are they for a given well over repeated trials? Are the averages over many wells?

The mean intensity (I_t) is just the average value of all of the pixels in a single well and is explained in lines 157-158. Therefore, there is a mean intensity for each well at every temperature (every image). Similarly, there is a normalized value Z_t' for each well at every temperature (each image, see lines 163-168).

To clarify this, we have now added "of *a single well*" to the caption of Figure 2b and "*for the same well as in b*" to the explanation of the caption for Figure 2c.

190 What is 'maximum standard deviation'?

We have now removed maximum standard deviation from the sentence and added a new sentence to explain the maximum standard deviation which reads: *"The maximum standard deviation taken as the temperature difference between the temperature fit and the individual well temperature was ±0.6 ˚C."* on lines 203-205.

196 -> The work here described in Section 3.2 is certainly well directed and quite extensive. However, it is surprising that nucleation temperatures of SA water are used instead of direct temperature measurements. It is the temperature of the water before, and at the instant, of nucleation that is most relevant. Direct temperature measurement of the water in the wells is not without its own difficulties (locating the sensors in the wells, sensor lead errors, etc.) but the variations in nucleation temperatures from well to well, even for SA water or other similar sample, are bound to be adding uncertainty to the calibration. What governed the decision to use nucleation temperatures to evaluate bias across the well-plate?

To directly measure the temperature of each well during an experiment, 96 thermocouples would be needed, which all can vary in temperature by about ± 2°C if they are not calibrated accurately. Alternatively, if the same thermocouple were used for all wells, 96 freezing runs would be needed to obtain only one temperature measurement for each well. Such a procedure is not feasible. Therefore, freezing runs performed with SA water were averaged, such that random variability cancelled out and systematic bias added up.

> **To assess the quality of this approach it would be useful to know how much variation in nucleation temperatures was observed for any given well within the 20 repeat tests. The two sources of variations - within a given well and among different wells - should be both presented and the sufficiency of the use of the median for each well thus evaluated.**
>
> We completely agree. The spread in the freezing temperature of the SA water in individual wells was indeed included in the original manuscript in the Appendix as Fig. A3, but was not mentioned in the main text. Although the distribution of freezing in the wells varied, the median was chosen as the most representative due to its definition as the center value of the distribution. Thus, it should be less sensitive to outliers than the mean. We have now added a reference to this figure on line 218 and reordered the Appendix figures accordingly, as such it is now Fig. A2.

226 Section numbering is off.

Thank you for pointing this out. We have now renumbered the section to be consistent with the rest of the manuscript (see line 242).

244 This standard deviation refers to the distribution of observed freezing temperatures among wells? Again, please distinguish between single well repetitions and variations among wells.

We have now added (lines 259-261) that the standard deviation here refers to "*the standard deviation in the observed freezing temperatures of the SA water experiments across all wells*"

246 The 50% fraction corresponds to the steepest point on the FF curve for SA water. But this is not a general result; other samples may have no such correspondence between the two measures.

This is absolutely true, but we chose the 50 % FF here as this is the most probable temperature at which the SA water freezes and therefore represents the best estimate of the bulk freezing properties of the water with a reduced influence from outliers and contamination. To clarify the reviewer concern we have now added the sentence (lines 263-264): *"Furthermore, by using the 50 % FF the influence of contamination and outliers is reduced."*

258 - 259 Fig. 4a shows, as expected, that the standard deviation varies according to the slope of the FF curve (sample size effect). Assigning this patters to the influence of ethanol circulation is likely to be incorrect.

Figure 4 shows that the deviation (bias) of each well in freezing temperatures from the median (panel a) and mean value (panel b) exhibit a non-random pattern. We see the ethanol circulation as the most likely explanation for such a pattern as the cooled ethanol circulates around the tray in a clockwise direction as indicated by the arrows in Fig. 4. We now clarify this on lines 222-224 of the revised manuscript.

More general point: to what extent in ethanol circulation predictable? This is a valid question in light of the flow being turbulent with the level control adding pulses of liquid.

In regards to the impact of the ethanol pulses on the ethanol circulation, it is important to point out that the pulses add very small volumes of ethanol and therefore likely have little impact on the circulation. In contrast, the change in bath level due to contraction during cooling likely has larger impacts on the flow in the bath due to changes of the exposed internal surface area of the bath. Therefore, the addition of ethanol likely makes the bath circulation more consistent. Regardless, no impact on the circulation was observed when observing the bath by eye with or without the use of the bath leveler.

304 -> The background correction via Eq. (10) is valid, but it is surprising that the correction is finally presented in terms of FF, via Eq. (11). Fitting a correction equation to $k_{bg}(T)$ would be more direct and more readily applicable to a variety of samples with different volumes and/or dilutions.

Indeed we use the method described by the reviewer, i.e. $k_{bg}(T)$ is used when correcting for the freezing background. The conversion to *FF* is just used to demonstrate how the background influences the *FF.*

342 -> Section 4.2 is well done. It is a good demonstration of the DRINCZ's capabilities. Was background correction applied?

Thank you for pointing this out. The results presented in section 4.2 are background corrected so we have added: *"and background corrected (using Eq. 11)"* to the sentence (lines 373-374).

373 -> Sections 4.3 to 4.5 introduce a topic beyond the description of the instrument. As has been amply shown in the extensive literature on the topic, analyses of snow samples are valid tools as inputs to the analyses of cloud processes, but with the attendant complicating factors partially discussed here. That current results vary within the range reported for other such measurements is due does demonstrate that the sampling techniques were adequate and that

the atmosphere is relatively conservative in the range of INP contents of snow. They do not substantially reinforce the validation of the instrument per se; that validation is more clearly supported by the calibrations and by the illite sample results. It is not stated (or it escaped me) whether the freezing analyses were done in the field or in the laboratory. This would be relevant to possibly show that the instrument is rugged enough for field use and that different setups do (or do not) effect the results.

We acknowledge that the measurements of field collected samples do not act as a validation of the technique. Rather they are added to the manuscript to show that the technique can be applied to field collected samples while providing the scientific community with additional observations of INP concentrations collected in snow samples.

In this case DRINCZ was not deployed in the field but the samples were shipped frozen to the laboratory in Zurich where they were stored frozen until the experiments were conducted. We have now adapted lines 403-404 to clarify that the samples were shipped frozen and the measurements with DRINCZ were conducted in Zurich by changing the sentence to read as: *"The samples were shipped and stored frozen until processed with DRINCZ at the Atmospheric Physics laboratory at ETH Zurich, to minimize any bacterial growth or changes due to liquid storage* (Stopelli et al., 2014)*."*

References:

Bigg, E. K.: The formation of atmospheric ice crystals by the freezing of droplets, Q. J. R. Meteorol. Soc., 79(342), 510–519, doi:10.1002/qj.49707934207, 1953.

Stopelli, E., Conen, F., Zimmermann, L., Alewell, C. and Morris, C. E.: Freezing nucleation apparatus puts new slant on study of biological ice nucleators in precipitation, Atmospheric Meas. Tech., 7(1), 129–134, doi:10.5194/amt-7-129-2014, 2014.

Review of "Development of the Droplet Ice Nuclei Counter Zürich (DRINCZ): Validation and application to field collected snow samples" by David et al.

General comment

In this manuscript the authors describe and characterise a large volume immersion mode drop assay (DRINCZ). The authors thoroughly characterise the horizontal temperature gradient across the 96 well plate in the system and recommend a correction which is of use to other instrumental setups. The authors report a ± 0.9 ˚C uncertainty for DRINCZ and go on to validate the instrument by comparing to literature data of NX-illite. A field study investigating snow melt samples is also undertaken which shows agreement (mostly) with previous snow melt measurements. The authors then relate the INP concentrations measured to airmass trajectories and propose scavenging of INP by precipitation led to the lowest INP concentrations measured.

This manuscript is well written and presents results which are of interest to the ice nucleation community. The manuscript is in the scope of AMT and I support its publication after the following comments have been properly addressed.

We thank the reviewer for the positive recommendation and for raising several points that we now address individually below and in the revised manuscript to make the paper clearer. Reviewer comments reproduced in bold and author responses in regular typeface. All line numbers in authors' response refer to revised manuscript.

Major comment

Although I like the manuscript and find the results of use to the ice nucleation community, I am unclear on the novelty of this instrument compared to others that have already been presented. The authors have acknowledged that the technique is based on the design of previous instruments. Is the method used to characterise and correct the horizontal gradients in the plate the only novelty? If so, I suggest this is made clearer in the final manuscript or that the unique traits of this instrument are further clarified.

We thank the reviewer for pointing this out. Indeed, the instrument is quite similar to previously developed drop freezing assays. New aspects are a method for determining horizontal gradients across the well plate and a fully automated data analysis, which only requires the user to enter a folder path name into a MATLAB function. We have now added the ease of data analysis as one of the benefits of DRINCZ by stating in the abstract (line 23): *"with a user friendly and fully automated analysis procedure."* Unfortunately, it is difficult to directly compare the ease of use and data analysis developed for DRINCZ relative to similar setups based on published papers, so we cannot be more specific.

The horizontal gradients of the plate have been characterised but the vertical gradients within the wells have not been explored. These should be discussed in the text. A reference to Beall et al. (2017) would be appropriate as they characterise the gradient within 50 µL droplets within wells with a similar profile (PCR plate).

It is very difficult to measure the vertical bias in a 50 µL well and this is also acknowledged in Beall et al. (2017). It is important also to note that in the setup of Beall et al. (2017), the polypropylene well tray is in contact with an aluminum block rather than the ethanol itself. This can lead to gradients due to the block, which would be negligible in our setup where the tray is in direct contact with the ethanol. Nevertheless, we have mentioned that the bath leveler can help reduce this issue on lines 176-180. We now reference Beall et al. (2017) in the revised manuscript to point out the possibility of vertical gradients in the wells and write that we attempt to avoid them by ensuring that the entire volume of solution inside the well is surrounded by ethanol. The addition to the text reads: *"It has been shown that large vertical gradients of up to 1.8 °C can exist between the bottom of a well and the air above it in block-based drop freezing setups (Beall et al., 2017). We anticipate vertical gradients to be reduced in DRINCZ due to the direct contact between the cooling medium (ethanol) and the well tray when the ethanol levels remains constant during cooling. Therefore, we incorporated a bath leveler composed of a level sensor and solenoid valve to ensure that the ethanol level remains constant."* (lines 176-180).

Figure 9 displays data for NX-illite dilutions. I find the text a little misleading in presenting the data as though there are only a "few" outliers for the 0.01wt% dilution. The vast majority of data for all three triplicates for this dilution give higher freezing temperatures than higher weight percent suspensions (at the same value of ns). This is in contradiction to what we expect of ns. I believe the source of this error is different to the uncertainties characterised in previous sections as the data is consistently offset to higher freezing temperatures. This issue is not seen (in most cases) in the dilutions for the snow melt study and suggests this discrepancy may be material dependent and related to the distribution of particles. Although the authors do mention this issue, the extent of the discrepancy between dilutions is glossed over in the text. I must stress that I do not believe this inconsistency in the dilutions is a result of an error in the instrument but rather an error as a result of the material or sampling method. With this said, the results should be presented in the text to acknowledge the true extent of this discrepancy.

The observed difference in the n_{sBET} values at the lowest weight percent compared with the higher concentrations falls within the uncertainty of the instrument (± 0.9 °C). Moreover, there is considerable variability between the triplicates performed with the same suspension concentrations. This can be seen in Fig. A4, where the *FF* curves of all NX-illite DRINCZ experiments are shown. In addition, we have updated Fig. 9 so that the difference between the triplicates of the NX-illite suspensions can be seen more easily. Nevertheless, we acknowledge that n_{sBET} of the 0.01 wt% NX-illite suspension is constantly above the n_{sBET} of the 0.05 and 0.1 wt% NX-illite suspensions. One reason for this might be that very few random freezing events occurring at warm temperature in the higher diluted sample may constantly increase cumulative active site densities to lower temperatures. However, based on the available data, we cannot exclude an effect due to dilution of a single stock suspension, which can lead to a bias compared with preparing suspensions of each concentration separately. We now discuss both possibilities in section 4.2 and reference the Harrison et al. (2018) study where issues arising from diluting a single stock suspension are discussed in detail. Nonetheless, we need to emphasize, that more investigations would be needed to establish the significance of the increased n_{sBET} observed at the lowest suspension concentration given the random variability between repetitions in such freezing experiments.

Minor comments

Line 67-77: Dilution is not the only means of changing the measurable range of INP. Concentrating the particles per droplet can also extend the range. I suggest this is added to the discussion.

This is a valid point. We add on line 71-73 after "aliquot": "*Alternatively, to explore freezing towards warmer temperatures, field samples (e.g. rain or snow samples) can be concentrated by evaporating a part of the sample water*."

Line 116: At what temperature does the ethanol bath start at and what temperature does it end, i.e. 0 ˚C to -30 ˚C. In addition to this, if the sample is added to an ethanol bath at 0 ˚C (as suggested by line 165) is the sample allowed time to equilibrate? If not, this could lead to thermal gradients not just horizontally across the plate but vertically in the wells (see major comment). I suggest adding information on the cooling profile of the bath to this section.

The wells are left to equilibrate to the bath temperature at 0°C for one minute before the experiment and cooling ramp is initiated. We have now added to the text on lines 107-108: *"The well tray is placed in the tray holder (Fig. A1) and left to rest for 1 min at 0°C before the experiment is started."*

Section 2.1.2: This describes the detection of freezing events in wells. Is this similar to other methods, e.g. (Stopelli et al., 2014)? Clarify what is different.

There is no appreciable difference in the detection method for identifying a freezing event relative to Stopelli et al. (2014). We have now added "*Similar to Stopelli et al, (2014)*" on line 123. However, rather than using a fixed intensity change as done by Beall et al, (2017), we use a normalized threshold of 0.6 as explained in the section. We have now clarified this difference on lines 168-170 by stating: "…*rather than relying on a fixed change in light transmission through the well as done by other drop freezing setups (Beall et al., 2017). This ensures that the initial freezing detection is independent of the absolute change in light transmission through a well*."

Section 2.2: What is the error of the sensor? What will be the fluctuation in the ethanol level? Do the authors consider it negligible?

There is no appreciable error in the sensor as it is a binary switch that either detects contact with or without the ethanol. As the sensor triggers the opening and closing of the solenoid valve to allow ethanol to flow into the bath, we expect fluctuations in the ethanol bath to be negligible.

Line 182-183: K type thermocouples can have large uncertainties, commonly ± 2.2 ˚C, compared to other thermocouple types (e.g. T type). Were these K type thermocouples calibrated other than by the manufacturer? What is the error of these? I suggest showing these errors in the figures (or an example of the errors).

Indeed, there can be differences between different thermocouples. That is why we did the temperature calibration using the same thermocouple in all five test locations. Therefore, the observed difference in the well temperature is based on the same thermocouple and not sensor dependent. As the temperature error reported is based on one thermocouple, the differences that we report can be

attributed to the locations of the wells in the tray. We did not calibrate the thermocouple in-house but rather compare the thermocouple temperature to the bath temperature of the chiller which is measured by a PT-100 temperature sensor. As such we have clarified this in the text by adding: "*The same thermocouple was used for all the well temperature measurements to avoid biases between different thermocouples.*" to lines 196-197

Line 183-184: Were the wells completely filled with ethanol or 50 µL? If completely filled does this represent the gradients that would be present in the wells and plate in a typical 50 µL experiment?

The wells were filled with 50 µL of ethanol to reproduce the experimental procedure used for DRINCZ freezing runs. We have now added *"50 µL of ethanol …"* to the text on line 197.

Section 3.2: The characterisation of the horizontal gradient across the plate is very useful for the community. However, has the vertical gradient within the wells been considered (see major comment)? This system uses a similar well profile to that used by Beall et al. (2017) who found that a vertical stratification of 0.5 ˚C can be found in wells in which the headspace (air above the wells) is ≥6 ˚C warmer. Please discuss this in the text and reference Beall et al. (2017) where appropriate.

It is very difficult to measure the vertical bias in a 50 µL well and this is also acknowledged in Beall et al. (2017). It is important to note that in the setup of Beall et al. (2017), the polypropylene well tray is in contact with an aluminum block rather than the ethanol itself. This can lead to gradients due to the block, which would be negligible in our setup where the tray is in direct contact with the ethanol. Nevertheless, as we now state in the response to the major comments, the bath leveler helps to reduce this issue (see response in major comments and revised manuscript line 175-180).

Also, you use the median freezing temperature of SA water to determine the offset in temperatures across the plate. Is there not a random probability of the SA water freezing at different temperatures without a temperature bias to start with? Would there also not be uncertainties due to accidental contamination in the individual wells during the setup of the experiment? Does this not create uncertainty in this experiment? What was the rationale for using SA water? If you were to use freezing temperatures (rather than direct measurements of the wells) then would something that froze more consistently at the same temperatures be a better standard to use, i.e. pollen has a narrow window for freezing.

We completely agree that there is a stochastic component to the freezing of the SA water. However, by averaging several experiments, the random variations cancel out while systematic bias adds up. Moreover, we calculate the precision of the instrument using the standard deviation of the temperature required for 50 % of the wells to freeze (see Section 3.3), which is less affected by random variability. In addition to minimize the effect of stochasticity, the 50% FF should also reduce the influence of contamination. Therefore we have added a sentence to Section 3.3 on line 263-264 stating: *"Furthermore, by using the 50 % FF the influence of contamination and outliers is minimized."* We chose SA water as the bias and precision standard for two reasons. First, the SA water is used in the majority of the experiments to prepare or dilute the samples. Therefore, its freezing curve needs to be

well known for background correction. Moreover, we use SA water as a reference sample to control the performance of DRINCZ and the constancy of the background. Therefore, we accumulated a large number of DRINCZ experiments with SA water available for closer analysis. Second, SA water has the lowest accessible freezing temperatures and at the lowest temperatures we expect the largest bias since the gradient between the air and the bath temperature is maximized.

Section 3.3: It is unclear to me why you assess the uncertainty of the instrument and combine this with the variability in the freezing temperature of SA water at this point. The water baseline in other studies, e.g. field-based studies, could potentially be worse (or better) than what you have done in these experiments. Should the experimental error as a result of the water impurities not be considered separately in respect to the particular experiment/environment?

Indeed, we use the freezing experiments performed with SA water for two purposes. First, in the laboratory we need to know the background freezing due to impurities present in the SA water for the samples that we prepare, collect or dilute with SA water (see Section 4.1). In the field, we also conduct background measurements with SA water in order to correct the observed IN concentrations. Second, we chose to use SA water as standard for quantifying instrument uncertainties because we accumulated a considerable number of SA water experiments performed by different users over a longer time period and therefore, we have the best statistics for this sample. In Sect. 3.3 we use the SA water experiments to establish instrumental uncertainties stemming from well-to-well temperature variations.

Section 4.2: There is no mention on how these suspensions/dilutions are made, how are the particles suspended? This could be particularly important given the results for NX-illite. I recommend adding this information in this section or the methodology.

Thank you for pointing this out. We have now added that: *An initial stock suspension of 0.1 wt % NX-illite was prepared and then diluted to produce additional mass concentrations of NX-illite of 0.05 and 0.01 wt%. The suspensions were manually shaken for 30 s, poured into a dispensing tray and then immediately pipetted into the well plate. Triplicates of each suspension concentration were investigated with DRINCZ..."* to lines 364-367 in Section 4.2.

Figure 9: it looks like the temperature intervals where no freezing events were observed are displayed in this figure, i.e. when binning the data, temperature intervals where 0 events were observed are still shown in the cumulative plots. As there are triplicates in this figure it makes it hard to discern which data points are real freezing events and which are artefacts of the binning process. This makes it difficult to interpret the data and the extent of the discrepancy between dilutions. If this is the case, I suggest removing the data points from the cumulative plots where there were no freezing events within a temperature interval for clarity.

Indeed, the plot shows triplicates for each weight percent but the values are not binned but just plotted at the observed temperature. We agree that the plot is a bit hard to interpret so we have remade the figure to help differentiate between the values reported in literature and shaded the triplicates to more clearly see the run-to-run variability at the different NX-illite concentrations. We have decided to keep all the observed n_{sBET} values since cumulative active site densities indeed remain at a constant value

when there is no freezing event in a given time interval. Moreover, constant values indicate that there is a poor data basis relying on rare freezing events.

Line 355-357: I would not definitively say that the ns is extended as expected. All three triplicates for the 0.01wt% dilutions are giving warming freezing temperatures than the higher weight percent suspensions (at the same value of ns). See major comment.

The purpose of the sentence is to state that by diluting the solution, we can observe freezing at lower temperatures and measure n_s at higher values. This is true even if the 0.01 wt% is slightly higher in n_s than the 0.05 and 0.1 wt% (within the instrumental uncertainty). Since we agree that we do not show a textbook case for the extension of n_s range by dilution, we have removed "as expected" from the sentence (376-377).

Line 357-358: In relation to the major comments, you state a few data points from the 0.01wt% suspension appear as outliers (and only at warmer temperatures), whereas all three runs for this dilution are shifted to warmer temperatures for the same value of ns. I suggest restructuring this paragraph to better represent the data and discuss the inconsistencies.

We have removed "a few data points" from the sentence to more accurately represent the higher n_{sBET} of the lowest weight percent solution at warm temperatures. As described in the response to the major comment, this discrepancy may be due to the presence of a few random active sites which lead to an increase in n_{sBET} that extends to lower temperatures or issues arising from diluting from a stock suspension. We have reworded lines 377-382 to: *"Similar to the observations of Harrison et al. (2018), the data points from the 0.01 wt. % solution appear as outliers at the warmest temperatures. However, it is not possible to determine if these outliers are due to random freezing events that occur at high temperatures and therefore produce elevated cumulative n_{sBET} values at lower temperatures or if they are due to an uneven distribution of the active sites in each aliquot that may result from diluting a single stock suspension rather than producing individual weight percent suspensions (Harrison et al., 2018)."* to offer an explanation for the observed divergence in the n_{sBET} between the wt% suspensions.

Line 358-360: In relation to the above, you reference that Harrison et al. (2018) used individually weighed suspensions rather than a single stock suspension to minimise the effect of uneven particle distributions. Why was this not done here if you believe this is the issue? This seems important as you are validating the instrument yet have inconsistent results on dilution.

As the discrepancies in n_{sBET} fall within the instrumental uncertainty of DRINCZ, looking for the true cause for the observed differences in the n_{sBET} values after dilution might be an over-evaluation of the data. Moreover, in addition to instrument uncertainties, there is also random variability in *FF* curves obtained from drop freezing assays. Indeed, when examining the *FF* curves shown in Fig. A4, there is considerable variability between triplicates performed with the same suspension concentration. Additionally, there are very few freezing events that occur at the highest temperatures in the 0.01 wt% suspension. Therefore, these high temperature freezing events that are responsible for the high cumulative n_{sBET} values of the 0.01 wt% suspension shown in Fig.9 can be random.

Line 362-363: At temperatures colder than -15 ˚C this doesn't seem to be the case (especially if you look at the 0.1-0.05wt% suspensions). There is just as good agreement with BINARY at colder temperatures (Hiranuma et al., 2015) but no comparison is made to this instrument.

We have now changed the sentence to state that the data falls between BINARY Leeds-NIPI and IR-NIPI as follows: *"Furthermore, considering the ± 0.9 ˚C uncertainty, depicted by the horizontal error bars, the differences between concentrations are not significant. They fall within the same range as the measurements of Beall et al, (2017) and between BINARY and Leeds-NIPI and IR-NIPI at colder temperatures (Fig. 9)."* (lines 384-385)

Line 374-375: Were the samples analysed at this field location or in the lab where the background freezing has been characterised? Were blank (pure SA water) experiments run at the time of these experiments to check the background signal had not changed?

Thank you for pointing this out. The samples were actually measured in the laboratory in Zurich and we have now clarified this by adding this information to lines (403-404): *"The samples were shipped and stored frozen until processed with DRINCZ at the Atmospheric Physics Laboratory at ETH Zurich to avoid any bacterial growth or changes due to liquid storage (Stopelli et al., 2014)."* Furthermore, we always ran an SA water blank before running DRINCZ on a measurement day to ensure that the background is the same and the system is working properly.

Technical comments

Line 41-43: This sentence needs restructuring/ re-wording as it is a bit clunky. E.g. an ice nucleating particle (singular) cannot get immersed in multiple cloud droplets.

Thank you, we have now made the sentence singular

Line 54: Should the word 'or' be in this sentence?

We have removed "or"

Line 57-59: No available technique can detect the lowest INP concentrations that are actually present in the atmosphere. I would suggest putting in a range of the INP concentrations detected with these techniques and rewording to say "to detect lower atmospheric INP concentrations".

We have now reworded the sentence to state: *"lower atmospheric INP concentrations."* (line 60). We have decided not to include a range as the measurable INP concentrations depend on the sampling method (e.g. time of sampling, impinger, filter etc.) as well as the measurement technique.

Line 102: What material is the 96-well plate made from? Polypropylene? I suggest adding here.

Thank you, we have now added polypropylene to the text.

Line 170-174: Suggest removing the terms 'potential' and 'possible' as adding 0 ˚C ethanol to ethanol at -30 ˚C will create a gradient, even if only small. Cooling the ethanol to 0 ˚C simply minimises this gradient.

Done

Line 201-201: Consider rephrasing this sentence.

We have now added a reference to Fig. 3 to clarify that the spread is referring to the temperature calibration.

Line 208-209: Consider rephrasing for ease of understanding.

We have now clarified that the observed bias is referring to the freezing temperature bias across the well plate.

Line 235-236: Harrison et al. 2018 is not a suitable reference in this instance. As I understand, they make individual temperature measurements for each well and as such, they take into account the horizontal gradient in temperature across the plate without the need for such a correction.

The Harrison et al. (2018) citation here is just meant as an example that such gradients do exist in block-based systems, which are observed in the IR-NIPI. Therefore we have changed the sentence (lines 251-252) to reflect this by adding *"… have been observed or modelled*."

Figure 2c: Perhaps label the peak which signifies initial nucleation

We have now clarified this in the figure caption by adding the sentence: *"The most intense peak corresponds to the ice nucleation temperature and the second most intense peak is due to the slow freezing of the solution after nucleation."*

Line 295: device not devices

Done

Line 307-309: This representation of the background you present is for DRINCZ in this particular lab environment. The baseline may change in field studies. I suggest rephrasing this section.

We have now added the preceding sentence (lines 323-324): *"Furthermore, an SA water sample is run as a standard at the beginning of each measurement day to ensure the system is operating correctly*." as to further motivate the use of SA water as a background and to ensure that the instrument background is reproducible in other settings.

Line 356: Suggest changing to "samples overlap to an extent"

Done

Line 445: missing bracket

Thank you.

Figure 9: the triangular symbols are hard to distinguish from one another. Suggest using different symbol shapes.

Thank you for pointing this out. We have now updated the symbols for clarity.

References:

Beall, C. M., Stokes, M. D., Hill, T. C., DeMott, P. J., DeWald, J. T. and Prather, K. A.: Automation and heat transfer characterization of immersion mode spectroscopy for analysis of ice nucleating particles, Atmos Meas Tech, 10(7), 2613–2626, doi:10.5194/amt-10-2613-2017, 2017.

Harrison, A. D., Whale, T. F., Rutledge, R., Lamb, S., Tarn, M. D., Porter, G. C. E., Adams, M. P., McQuaid, J. B., Morris, G. J. and Murray, B. J.: An instrument for quantifying heterogeneous ice nucleation in multiwell plates using infrared emissions to detect freezing, Atmospheric Meas. Tech., 11(10), 5629–5641, doi:https://doi.org/10.5194/amt-11-5629-2018, 2018.

Stopelli, E., Conen, F., Zimmermann, L., Alewell, C. and Morris, C. E.: Freezing nucleation apparatus puts new slant on study of biological ice nucleators in precipitation, Atmospheric Meas. Tech., 7(1), 129–134, doi:10.5194/amt-7-129-2014, 2014.